RTO-TR-075(II)
AC/323(SET-015)TP/21

RTO-TR-075(II)

NORTH ATLANTIC TREATY ORGANISATION

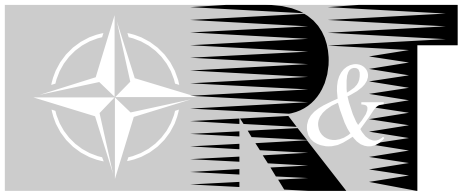

RESEARCH AND TECHNOLOGY ORGANISATION

BP 25, 7 RUE ANCELLE, F-92201 NEUILLY-SUR-SEINE CEDEX, FRANCE

RTO TECHNICAL REPORT 75(II)

Experimental Assessment Parameters and Procedures for Characterisation of Advanced Thermal Imagers

(Paramètres et procédures d'évaluation expérimentale pour la caractérisation d'imageurs thermiques avancés)

Final Report of Task Group SET-015/RTG of the Sensors and Electronics Technology Panel.

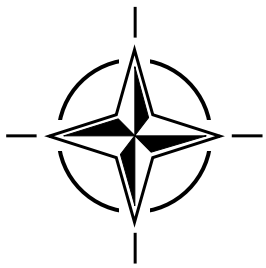

Published February 2003

Distribution and Availability on Back Cover

This page has been deliberately left blank

Page intentionnellement blanche

RTO-TR-075(II)
AC/323(SET-015)TP/21

NORTH ATLANTIC TREATY ORGANISATION

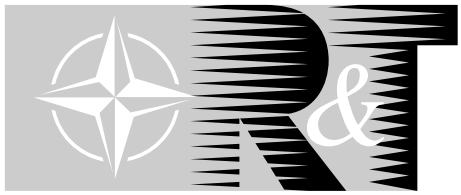

RESEARCH AND TECHNOLOGY ORGANISATION

BP 25, 7 RUE ANCELLE, F-92201 NEUILLY-SUR-SEINE CEDEX, FRANCE

RTO TECHNICAL REPORT 75(II)

Experimental Assessment Parameters and Procedures for Characterisation of Advanced Thermal Imagers

(Paramètres et procédures d'évaluation expérimentale pour la caractérisation d'imageurs thermiques avancés)

Final Report of Task Group SET-015/RTG of the Sensors and Electronics Technology Panel.

The Research and Technology Organisation (RTO) of NATO

RTO is the single focus in NATO for Defence Research and Technology activities. Its mission is to conduct and promote cooperative research and information exchange. The objective is to support the development and effective use of national defence research and technology and to meet the military needs of the Alliance, to maintain a technological lead, and to provide advice to NATO and national decision makers. The RTO performs its mission with the support of an extensive network of national experts. It also ensures effective coordination with other NATO bodies involved in R&T activities.

RTO reports both to the Military Committee of NATO and to the Conference of National Armament Directors. It comprises a Research and Technology Board (RTB) as the highest level of national representation and the Research and Technology Agency (RTA), a dedicated staff with its headquarters in Neuilly, near Paris, France. In order to facilitate contacts with the military users and other NATO activities, a small part of the RTA staff is located in NATO Headquarters in Brussels. The Brussels staff also coordinates RTO's cooperation with nations in Middle and Eastern Europe, to which RTO attaches particular importance especially as working together in the field of research is one of the more promising areas of initial cooperation.

The total spectrum of R&T activities is covered by the following 7 bodies:

- AVT Applied Vehicle Technology Panel
- HFM Human Factors and Medicine Panel
- IST Information Systems Technology Panel
- NMSG NATO Modelling and Simulation Group
- SAS Studies, Analysis and Simulation Panel
- SCI Systems Concepts and Integration Panel
- SET Sensors and Electronics Technology Panel

These bodies are made up of national representatives as well as generally recognised 'world class' scientists. They also provide a communication link to military users and other NATO bodies. RTO's scientific and technological work is carried out by Technical Teams, created for specific activities and with a specific duration. Such Technical Teams can organise workshops, symposia, field trials, lecture series and training courses. An important function of these Technical Teams is to ensure the continuity of the expert networks.

RTO builds upon earlier cooperation in defence research and technology as set-up under the Advisory Group for Aerospace Research and Development (AGARD) and the Defence Research Group (DRG). AGARD and the DRG share common roots in that they were both established at the initiative of Dr Theodore von Kármán, a leading aerospace scientist, who early on recognised the importance of scientific support for the Allied Armed Forces. RTO is capitalising on these common roots in order to provide the Alliance and the NATO nations with a strong scientific and technological basis that will guarantee a solid base for the future.

Published February 2003

ISBN 92-837-1095-9

Printed by St. Joseph Print Group Inc.
(A St. Joseph Corporation Company)
1165 Kenaston Street, Ottawa, Ontario, Canada K1G 6S1

Experimental Assessment Parameters and Procedures for Characterisation of Advanced Thermal Imagers

(RTO TR-075(II) / SET-015)

Executive Summary

The infrared community has entered an era where staring imagers are becoming the norm and not the exception. Staring array sensors are quickly making their way into target acquisition and surveillance/reconnaissance applications. The large detector characteristics and improved optical quality of these systems make for undersampled image transfer with high sensitivity. The classical MTF and MRTD resolution and visual performance parameters, respectively, do not exist for undersampled imagers. In addition, the higher sensitivity of these systems requires that new noise measures be implemented.

The objective of this study undertaken by the RTO SET Panel Task Group 12 (TG12) was the development and investigation of experimental assessment parameters and measurement techniques required for characterising advanced staring or micro-scanned thermal imagers. This study is complementary to a previous TG12 report entitled “Modelling of Undersampled Infrared Imaging Systems” which is published as a separate RTO Publication (RTO-TR-075(I)).

TG12 collectively and TG12 member countries have developed and investigated a number of measures and measurement techniques to characterise advanced thermal imagers. They are presented in this report. These measures and techniques allow assessment of basic, system-relevant sensor parameters, such as spatial resolution and noise, as well as overall sensor performance.

Numerous measures and techniques are now available to characterise spatial information transfer and noise in advanced thermal imagers. Also, various figures of merit and measurement techniques were developed to assess the overall device performance. Some of the new figures of merit, such as Minimum Temperature Difference Perceived (MTDP), are evolutions of the classical MRTD figure of merit. Other techniques for overall performance assessment use triangles and double-slits as test patterns. These techniques were developed to reduce possible measurement inaccuracies introduced by the subjective nature of assessment techniques which use standard 4-bar test patterns, and have benefits which should further be investigated. All figures of merit will remain in use for further evaluation, which is strongly recommended.

Techniques to assess overall device performance without human observer respond to the continued interest of the IR community to have fast and reliable assessment techniques. Such techniques are still under development.

Summary of Recommendations:

1. Establish a board of experts and an AGGRESSIVE program for developing/evaluating techniques for modelling, measurements, and range performance predictions of undersampled imagers with the goal of drafting STANAG(s) for imager performance. Realize that this is a significant effort that requires nations to participate in laboratory evaluations of techniques, so nations must be willing to invest time and effort in a development/evaluation program. It should not be the part-time goal of a Technical Group.

2. Note that for the immediate future, there will be mis-applications of the current STANAG methods to undersampled imagers. Staring and scanning infrared sensors are unfairly compared using the current STANAG methods. It is recommended that the MTDP method or the NVTherm/DMRT (dynamic MRTD) method be used until further evaluation can be performed.

3. Standardise definitions and measurement techniques for assessing resolution and sensitivity of advanced imagers.
4. Review and update STANAGs 4347, 4349, and 4350 for use with well-sampled imaging systems. There have been numerous improvements in MRTD modelling, measurements, and range performance over the past 10 years.
5. Develop “objective” techniques to assess overall device performance without human observer. This is in the continued interest of the IR community and hence should be further encouraged.

Paramètres et procédures d'évaluation expérimentale pour la caractérisation d'imageurs thermiques avancés

(RTO TR-075(II) / SET-015)

Synthèse

Pour les spécialistes de l'infrarouge, l'époque qui commence est celle où les imageurs à mosaïque infrarouge sont maintenant la norme et non plus l'exception. Aujourd'hui, les capteurs fixes trouvent de plus en plus d'applications dans les domaines de l'acquisition d'objectifs et la surveillance/la reconnaissance. Les grandes caractéristiques de détection et la qualité optique améliorée de ces systèmes permettent de réaliser des transferts d'images sous-échantillonnées avec une grande sensibilité. Les paramètres de résolution et de performance visuelle des MTF et MTRD classiques n'existent pas pour les imageurs sous-échantillonnés. En outre, la plus grande sensibilité de ces systèmes nécessite la réalisation de nouvelles mesures de bruit.

Cette étude, effectuée par le groupe de travail No. 12 de la commission SET de la RTO, a eu pour objectif d'examiner et de développer des paramètres expérimentaux d'évaluation, ainsi que des techniques de mesure pour la caractérisation d'imageurs thermiques à mosaïque infrarouge et à micro-balayage avancés. Cette étude vient compléter le précédent rapport de TG12 intitulé « La modélisation de systèmes d'imagerie infrarouge sous-échantillonnés » qui est édité sous forme de la publication RTO-TR-075(I).

TG12, de façon collective, et les pays membres de TG12 de façon individuelle, ont examiné et développé un certain nombre de mesures et techniques de mesure qui permettent de caractériser les imageurs thermiques avancés. Elles sont présentées dans ce rapport. Ces mesures et techniques permettent d'évaluer les paramètres de base des systèmes de détection, tels que la résolution spatiale et le bruit, ainsi que les performances globales des capteurs.

Un grand nombre de mesures et de techniques sont désormais disponibles pour la caractérisation du transfert spatial des informations et du bruit dans les imageurs thermiques avancés. Aussi, différents facteurs de qualité et techniques de mesure ont été développés afin d'évaluer les performances globales des dispositifs. Certains nouveaux critères de mérite tels que la différence minimale de température perçue (MTDP), sont des évolutions du facteur de mérite MRTD classique. D'autres techniques d'évaluation des performances globales font appel à des mires composées de triangles et de trous de Young. Ces techniques ont été élaborées dans le but de réduire d'éventuelles erreurs de précision introduites par la nature subjective des techniques d'évaluation basées sur des mires classiques à quatre barres, et méritent un examen plus approfondi. Tous les facteurs de mérite seront retenus aux fins d'évaluations ultérieures, qui sont, d'ailleurs, fortement recommandées.

Des techniques destinées à évaluer les performances globales des systèmes, sans la présence d'observateurs humains répondraient à la demande exprimée par la communauté IR, de techniques d'évaluation rapides et sûres. Elles sont encore en cours de développement.

Résumé des recommandations

1. Un comité de spécialistes, avec un programme dynamique de développement/d'évaluation de techniques de modélisation, de mesure, et de prévision de performances en portée d'imageurs sous-échantillonnés, en vue de la rédaction de STANAG's sur les performances des imageurs devrait être établi. Il faut savoir que ceci demandera des efforts significatifs. En particulier, il faudra demander aux pays de participer à des évaluations en laboratoire et ils devront donc être prêts à s'investir pour exécuter un programme de développement/d'évaluation. Il ne devrait pas s'agir d'un projet à temps partiel pour un groupe technique.

2. Il faut noter qu'à court terme, il faut s'attendre à des applications erronées des méthodes préconisées par les STANAGs actuels. Les comparaisons qui sont actuellement faites entre les capteurs à mosaïque infrarouge et les capteurs à balayage infrarouge, selon les méthodes préconisées par les STANAGs, ne sont pas justes. En attendant d'autres évaluations, il serait préférable d'appliquer soit la méthode MTDP, soit la méthode NVTherm/DMRT (MRTD dynamique).
3. Les définitions et les techniques de mesure pour l'évaluation de la résolution et la sensibilité des imageurs avancés devraient être normalisées.
4. Les STANAGs 4347, 4349 et 4350 pour application aux systèmes d'imagerie correctement échantillonnés doivent être revus et mis à jour. De nombreuses améliorations ont été apportées à la modélisation, aux mesures et aux performances en distance du MRTD au cours des dix dernières années.
5. Il s'agit maintenant d'élaborer des techniques « objectives », permettant d'évaluer les performances globales des systèmes sans intervention humaine. Une telle démarche conforterait les intérêts à long terme des spécialistes de l'IR et devrait être encouragée.

Click inside the blue boxes to view the corresponding section

Contents

Chapter 1

Introduction

The battle-winning capability provided by infrared technology has been published in recent years by worldwide media coverage of major military conflict. The advantages provided by these technologies are now well established and understood by military strategists.

To respond to the demand for product superiority in infrared technology, a new generation of advanced infrared focal plane array detectors (FPA) have been developed in NATO, most notably in France, Germany, the UK and US. Many different types of FPAs are now available from uncooled arrays (e.g. bolometer) to cooled arrays using a wide range of photosensitive materials and technologies (e.g. CMT, InSb, PtSi, QWIP).

These advanced state of the art IR technologies are now becoming available in a number of IR systems either entering service now, or planned to enter service in the near future. They are offering increased performance with the added benefits of improved reliability and lower life cycle costs.

In response to the perceived need to coordinate a common approach to the assessment and characterisation of these advanced systems, TG12 was tasked with developing an approach to the analysis of advanced IR FPA systems. This report is the advances produced by TG12 in assessing these IR systems. Performance measures developed for 1st generation thermal imagers that can also be used without modifications for advanced systems were not addressed and are not reviewed in this paper.

The purpose of this report is to inform the NATO community of the conclusions of NATO RTO-SET/TG12's work concerning the development of a common approach to the experimental characterisation and assessment of advanced IR systems, to indicate areas where further convergence of ideas and techniques is needed, and to recommend the preparation of future NATO STANAGs covering the definition, assessment and characterisation of advanced IR imagers in those areas where formal agreement now exists within TG12.

In a companion report[1] we inform the NATO community on the status of the range performance modelling of advanced thermal imagers, and the activities TG12 has undertaken to validate current target acquisition models.

1.1 DEFINITION OF ADVANCED SYSTEMS

It is important at the outset to define clearly what TG12 means by an advanced IR system and what the group has excluded from its current study. In the context of the assessment and characterisation studies conducted within the group, an advanced system has been defined as one that utilises infrared focal plane arrays where the detector signals are integrated on the chip and multiplexed before read-out. Inherent feature of advanced systems is that the information is sampled in both directions.

Examples of advanced infrared focal plane arrays include two-dimensional arrays of e.g. 640 x 512 detectors and linear detector arrays with e.g. 576 x 7 detectors. Two-dimensional arrays stare at the infrared scene whereas linear detector arrays are scanned mechanically by the use of mirrors etc across the FOV. Further distinction may be made between two-dimensional detector arrays that are purely staring and those that are micro-scanned (or dithered).

The generic type of 'advanced' infrared imager considered by TG12 is shown in Fig. 1.1. It is a staring imager with a two-dimensional FPA. This type of imager is undersampled and has non-neglectable fixed pattern noise. These features, which are described in Section 2, constitute the new challenges in assessing advanced systems.

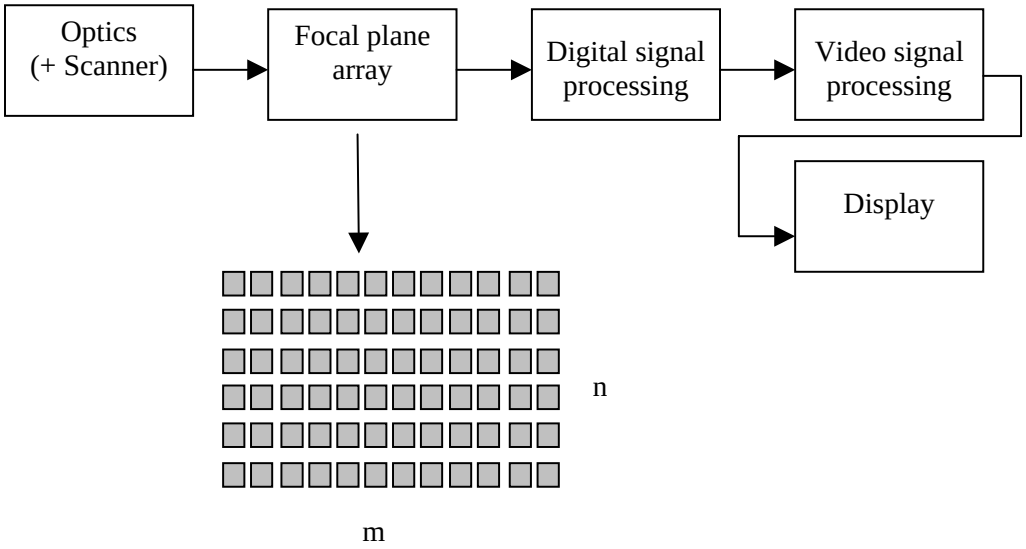

Fig 1.1: Generic type of an advanced system as studied by TG12.

Advanced system includes cooled and uncooled technologies and the many different silicon multiplexers and charge storage and read-out techniques, e.g. CCD, CMOS etc. The techniques and methodologies developed and tested by the group are designed to be generic and are therefore not sensitive, for example, to the type of silicon multiplexer used, or the infrared diode structure as this would restrict the usefulness of the tests and techniques to a narrow range of technologies.

The group has not extended the study to an analysis of focal plane arrays with retinal or adaptive processing on the focal plane neither are functions such as on focal plane ADC considered. These areas were beyond the remit of the group.

1.2 STRUCTURE OF THE REPORT

The next sections are devoted to the exposition of measures, figures of merit and measurement techniques developed or studied by TG12 and its predecessor group, RSG16 of AC/243, and used to characterise advanced systems. They are divided in three main categories, which are treated in separate sections.

Section 2 describes measures characterising the spatial resolution of advanced imagers. First it is outlined why the system MTF cannot be used to characterize the spatial resolution of undersampled imagers. The newly developed assessment parameters and measurement techniques that take into account the special requirements imposed by the sampling process in advanced systems are considered here.

Section 3 describes measures characterising the thermal sensitivity of the imager. Attention is given to characterize the temporal and spatial noise in advanced FPA systems including bad pixel characterization.

Section 4 deals with figures of merit characterising overall device performance: The sampling of the detector signals as well as spatial noise due to non-uniformities affect the performance of advanced imagers. Overall figures of merit that cope with these features are presented and compared to the classical MRTD figure of merit. Subjective measures as well as objective techniques are addressed.

The measured are discussed in Section 5. General conclusions and suggestions for further research and recommendations are given in Section 6. For more technical information, original papers are reported in the REFERENCES.

Chapter 2

Assessment of Spatial Information Transfer

2.1 THE LIMITS OF THE MTF CONCEPT

2.1.1. The MTF concept

The ability to reconstruct spatial information of a scene is related to the spatial resolution of the imager. Tools to describe the spatial resolution of thermal imagers are derived from linear filter theory.

Assuming that the imager is a linear, space- and time-invariant system, the spatial resolution of the imager is described by its *Point Spread Function*, PSF, and its *Optical Transfer Function*, OTF, which is the Fourier transform of the PSF. Modulus and phase of the OTF are defined as *Modulation Transfer Function*, MTF, and phase transfer function, PTF, of the system. PSF and OTF/MTF are two-dimensional functions.

The *Line Spread Function*, LSF, is a one-dimensional function. It is given by integrating the PSF in one direction:

$$LSF(x) = \int PSF(x,y)dy \quad .$$

The Fourier transform of the LSF is the one-dimensional OTF, its modulus the one-dimensional MTF. Most measurement techniques derive the one-dimensional MTF from an LSF measurement using a slit source as test pattern. The PTF is not used to assess thermal imager performance.

The MTF is a powerful parameter to assess linear and space-invariant imaging systems since the MTF of a complex system is the product of the MTFs of its incoherently coupled components. Theory and measurement of the MTF of imaging systems is treated in a STANAG. [2] [3]

2.1.2. Applicability of the MTF concept to advanced thermal imagers

In order to apply the MTF concept to a thermal imager it must behave like a *linear* and *isoplanatic* system. Within a limited range of scene temperatures the imager always has a linear response to the incoming signal. This linear range depends on the gain and offset setting of the imager and can be derived from the measurement of the Signal Transfer Function (SiTF). [4]

The imager is isoplanatic if the point spread function is space-invariant; i.e. it does not change within the field of view (FOV), or at least part of it. While first generation (scanning) imagers with analog signal processing can be considered space-invariant in scan direction, advanced thermal imagers, especially staring imagers, usually are not space-invariant in any direction. This is due to the insufficient sampling of spatial information in both directions. Individual components of the imager, however, and groups of components can be considered space-invariant.

With respect to the MTF characterization, imager components, which act on the signal before sampling, can be considered as *prefilter* components. Imager components that act on the signal after sampling can be considered as *postfilter* components. Normally, these components are space-invariant and hence can be described by MTFs:

Prefilter MTF: The product of the MTFs of all incoherently coupled prefilter components. (E.g. front optics and detector elements).

Postfilter MTF: The product of the MTFs of all incoherently coupled postfilter components (e.g. video and display).

The MTF concept, however, is not suited to assess the spatial transfer characteristics of an advanced imager as a whole. This is described in more detail in the next paragraphs. Alternative descriptors are needed.

2.1.3. The sampling of information in advanced imagers

A two-dimensional focal plane detector array is a device that consists of detector elements with a particular size and shape, separated by a given distance, see Fig. 2.1. The distance between the centres of two adjacent detectors is the detector *pitch*.

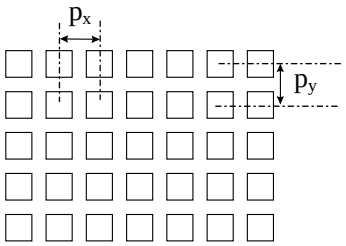

Fig 2.1: View of the physical structure of a two-dimensional FPA

The *sampling distances* are the distances between subsequent horizontal and samples taken by the imager. In staring imagers the sampling distance in either direction equals the detector pitches. In micro-scanned imagers, the sampling distance in either direction is given by the pitch divided by the number of micro-scan steps in that direction. The *sampling frequency* is the inverse of the sampling distance.

2.1.4. Sampling and undersampling

The sampling theorem deals with the capacity of a sampled system to transmit information. In case of optical information this capacity means the ability of the system to reproduce the spatial frequencies that form a particular scene. The principal result of this theorem is to establish an upper limit for frequencies that can be faithfully transmitted and reconstructed from the original signal. This limit is often called the *Nyquist frequency* which is given by,

$$f_{Nyquist} = 1/2b\ .$$

where b is the sampling distance.

Mathematically, in sampling systems, the spectrum of the original signal is replicated at intervals f_s, where f_s is the sampling frequency, see Fig. 2.2. A signal at frequency f re-appears as a pseudo-signal at the frequencies $nf_s - f$ and $nf_s + f$, with m any integer number.

If the spectrum of the original signal contains frequencies higher than the Nyquist frequency, the original spectrum and the replicated spectra overlap. In such a case, the original signal can by no means be reconstructed faithfully. An imager who allows that the original spectrum overlaps with the back-folded spectrum is called *undersampled*. The imager is undersampled if the prefilter MTF is not equal to zero at Nyquist frequency.

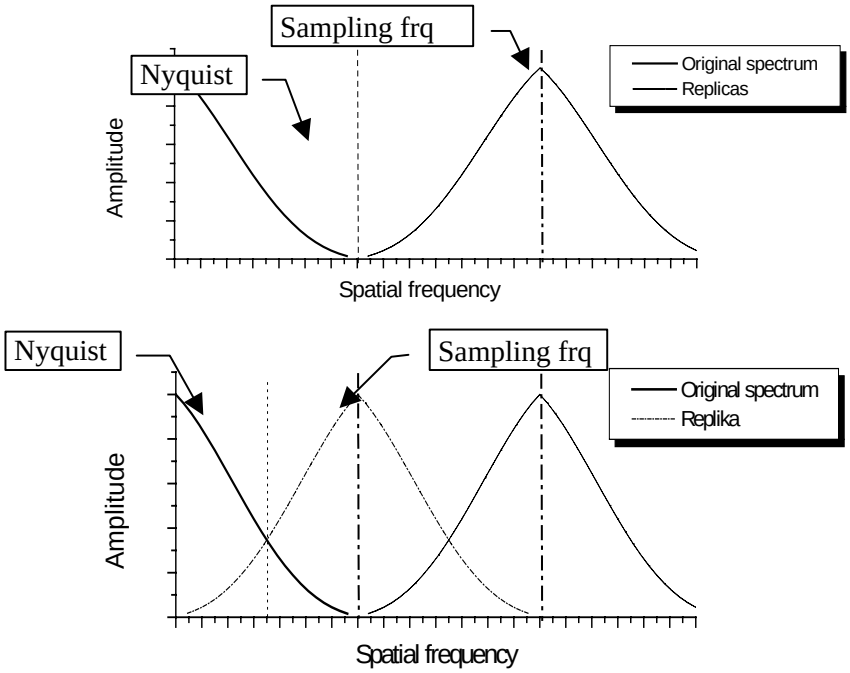

Fig 2.2: The spectrum of a sampled signal: The original spectrum is replicated at multiples of the sampling frequency. If the prefilter MTF of the imager is band-limited at a frequency lower than the Nyquist frequency (top figure) the image is properly sampled. If this is not the case (bottom figure) the imager is *undersampled*.

The original signal can be reconstructed faithfully only if (1) the signal is band limited at a frequency lower than the Nyquist frequency and if (2) a postfilter is used which eliminates all back-folded frequency components higher than the Nyquist frequency. If these conditions are not met, artefacts appear in the reconstructed image. This is called *aliasing*.

The imager is isoplanatic, or shift invariant, if the "shape" of the PSF does not depend on the particular position on the object plane. If the object to be viewed is moved, the image remains the same. This is not true for an undersampled imager. The PSF depends on the position in object space; the system is not shift invariant. More specifically, the PSF depends on the position of the point source relative to the detector array. This relative position is called the *phase*, see Fig. 2.3.

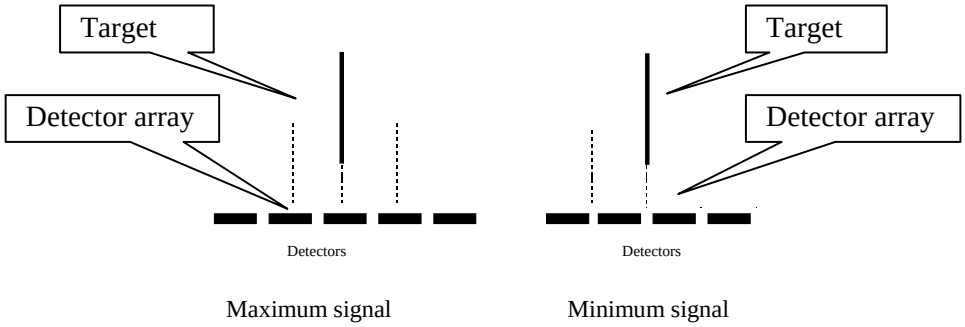

Fig 2.3: Different phases between target and detector array produce different signals.

Due to the periodicity of the detectors in the array, the changes in PSF due to phasing effects are periodic, too. A point source is viewed under the best conditions when the centre of the point is in phase with the centre of a detector. The worst case is given when the point source is located between the

detector elements. Generally, contrast and modulation of a signal depend on its phase with respect to the detectors.

2.1.5. New performance measures and techniques

Although in case of undersampling, the overall *system MTF* is not defined and hence cannot be measured, the MTF concept still can be used to characterize part of the imager.

The *prefilter MTF* plays an important role in the TRM3[5] and NVTherm[6] models. If measured, it allows to calculate the *actual* amount of in-band aliasing of the imager (NVTherm) and to simulate the actual sampling of information (TRM3). The *postfilter MTF* allows assessing how the digitised signals are actually reconstructed. If both pre- and postfilter MTFs are measured the amount of out-of-band aliasing in the displayed image can be calculated (NVTherm) and the image of an input signal can be reconstructed (TRM3).

Special techniques are required and were developed to perform MTF measurements in undersampled imagers. These techniques are described in the following paragraphs. For the overall assessment new concepts were developed (AMOP and double-slit technique) that are described in the remaining paragraphs of this section.

2.2 BEST AND WORST 'MTF'

In case of isoplanatic systems the LSF can be measured by either moving the test source and analysing the signal at a fixed position or vice versa. The result is the same and leads to the (one-dimensional) MTF.

The standard technique to measure the horizontal LSF in 1st generation thermal imagers with analog signal output is to keep the line source fixed and to record and to analyse the output signal. The modulus of the normalized Fourier transform of this signal gives the system.

If this procedure is applied to advanced undersampled thermal imagers the measured signal depends on the phase between test slit and detector array, as described in the previous paragraph. The technique is still used by some laboratories to characterise the performance of undersampled thermal imagers. Normally, measurements are made at best and worst phase (see above). The modulus of the Fourier transform of the measured and normalised line signal is designated *best 'MTF'* and *worst 'MTF.'*

Although these measurements are no MTF measurements useful information can be extracted: The shape of both best and worst MTF is governed by the postfilter, most especially by the reconstruction function. The type of reconstruction function used can be easily estimated from this measurement. Also, comparison of best and worst MTF allows qualitative assessment of the undersampling of the imager. In addition, from the signal difference between the peak signals at best and worst phase gives a measure for the *effective filling factor* of the imager.

2.3 SCANNING SLIT METHOD

In the Scanning slit method[7] the slit source is moved and the reproduced line signal is analysed at a fixed position in the output signal, whether digital or video output, see Fig. 2.4. The signal at this position is recorded as function of the slit displacement, which gives the line, spread function.

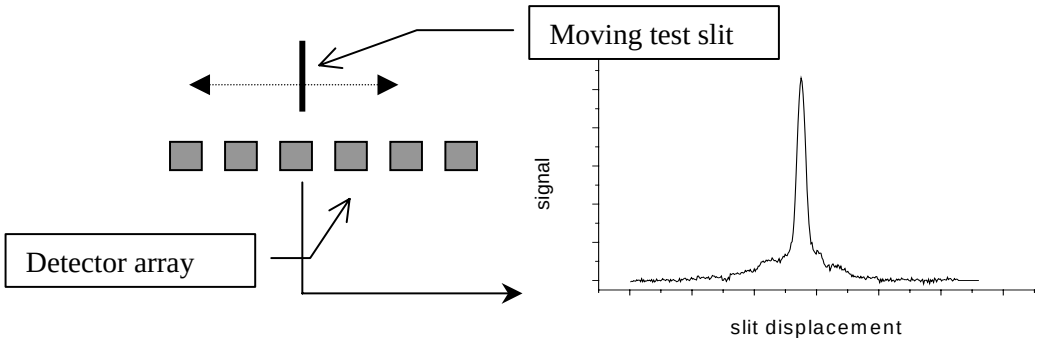

Fig. 2.4: Scanning slit method. The test slit is moved and the signal is analyzed at a fixed position in the output signal. The signal as function of the slit displacement gives the line spread function.

The method can be applied to all types of sampled imagers, scanning, staring or micro-scanned. The advantage of this method is that, with few exceptions, the measurement result is unique and can be interpreted: If the measurement is made in the digital domain, the measurement leads to an MTF, which is given by

$$MTF_{scanning\ slit} = MTF_{pref} \cdot MTF_{dig}$$

where MTF_{pref} is the MTF of the prefilter and MTF_{dig} the MTF of any digital filter used. Undersampled imagers usually have no digital filter and, therefore, the measurement normally gives the prefilter MTF.

If measured in the video signal the technique leads to a result, which is given by:

$$MTF_{scanning\ slit} = MTF_{pref} \cdot MTF_{dig} \cdot c(r)\,,$$

where c is a function of spatial frequency r. c depends on the postfilter MTF and is equal to one if the postfilter MTF does not introduce additional signal degradation.

One advantage of the scanning slit technique is that using just one single detector as probe residual detector non-uniformities do not affect the measurement. The displacement of the slit source can be made with very small increments, thus improving the accuracy of the measured line spread function.

In order to obtain a sufficiently high signal-noise-ratio the signal at each slit position must be measured repeatedly in subsequent frames and averaged. If the measurement is made in the analog video signal no expensive digital data acquisition equipment is needed.

2.4 DMTF METHOD (DISCRETE MODULATION TRANSFER FUNCTION)

The DMTF method[8] is preferably applied to staring imagers with digital output. The basic approach is to record the test slit image at different equidistant phases and to interweave the signal recorded at each phase position, thus increasing the effective sampling frequency.

Assume that the pitch in the focal plane array be b. The sampling frequency is then 1/b. The test slit, or the imager, is moved in n discrete steps at step intervals Δx given by

$$\Delta x = \frac{b}{n}$$

At each step the test slit image is recorded at the digital output. The recorded sampled image signals are then interwoven. This gives a new sampled test image signal with a sampling distance of Δx or a

sampling frequency that is n times higher than the original sampling frequency of the imager. The approach is illustrated in Fig. 2.5.

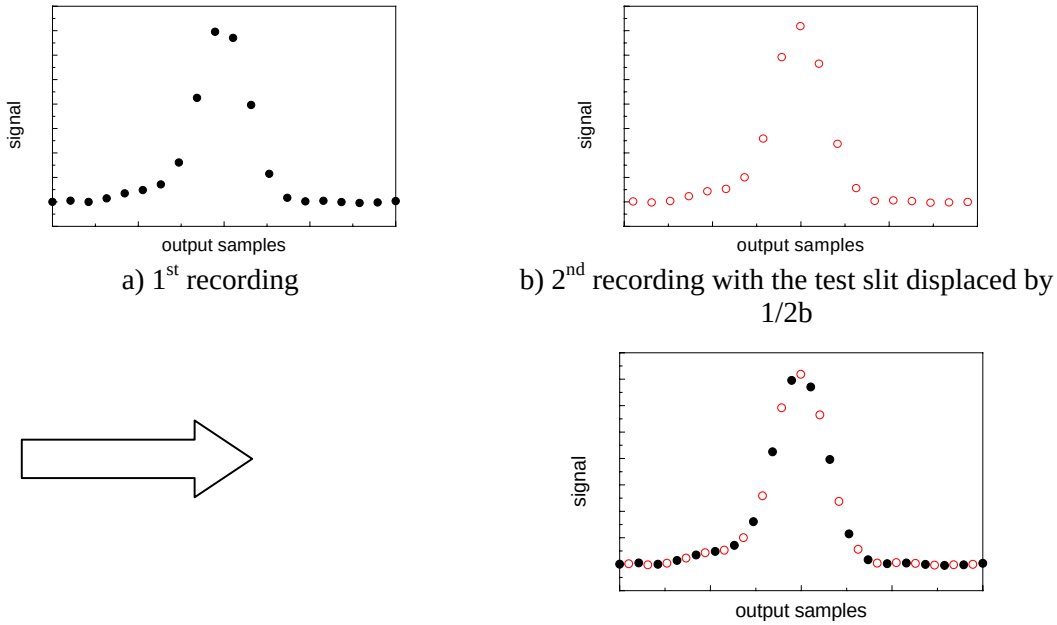

a) 1st recording

b) 2nd recording with the test slit displaced by 1/2b

c) Interwoven signal

Fig. 2.5: Illustration of the DMTF method with n=2. The test image signal is recorded at two equidistant phase positions (top part). The two recordings are then interlaced (bottom right). This gives a sampled test slit image with a sampling frequency that is two times higher than the original one.

The number of steps n is chosen in such a way that the Nyquist criterion is satisfied for the highest frequency transmitted by the system (usually the optics cut-off).

The DMTF method is a fast technique to assess staring or micro-scanned imagers, preferably at the digital video output. Contrary to the scanning slit technique, several detectors contribute to the measured line signal. It is assumed that these detectors have the same performance. Residual detector non-uniformity must be removed in order to obtain an un-biased signal.

2.5 THE TILTED SLIT METHOD

A slit (or edge) is positioned at a small angle relative to the detector columns or lines, see Fig. 2.6. Assume that the slit is tilted by an angle α relative to a horizontal line of detectors. Between the centres of two adjacent detector elements the slit is displaced in vertical direction by Δy, with

$$\Delta y = b \cdot tan(\alpha)$$

where b is the horizontal detector pitch. The output signal is analysed in horizontal direction.

With this technique one obtains samples of the vertical line spread function at sample intervals Δy. If the slit is tilted relative to a vertical line of detectors the output signal is analysed in vertical direction to obtain samples of the horizontal line spread function. The smaller the tilt angle α, the smaller is the sample interval. Fig. 2.7 shows the image of a tilted slit as an example.

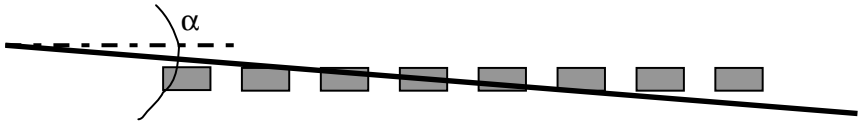

Fig. 2.6: The tilted slit method. The test slit (or edge) is tilted relative to the orientation of the detector elements.

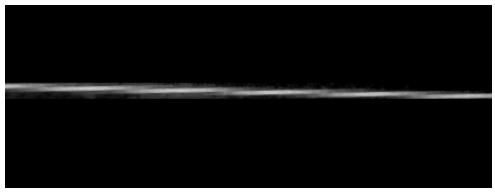

Fig. 2.7: Example of an image taken with a tilted slit.

The tilted slit (or edge) method is a fast technique. The measurement can be made at the digital video output or in the analog video signal. The tilt angle α must be known with high accuracy. Residual detector non-uniformities affect the signal the same way as in the DMTF method.

2.6 GLSF METHOD (GENERALIZED LINE SPREAD FUNCTION).

The GLSF technique[9] uses a periodic test pattern of thin lines which are separated by a distance d, see Fig. 2.8 This distance is chosen such that

$$d = \left(n + \frac{1}{2}\right) \cdot s$$

where s is the sampling distance and n an integer that depends on the cut-off frequency of the front optics of the imager. The frequency spectrum of this test pattern has discrete values at frequencies r_i with

$$r_i = \frac{i}{\left(n + \frac{1}{2}\right) \cdot s} \text{ with i} = 1,2,3,...$$

Due to the factor 1/2 the back-folded frequency spectrum does not interfere with the original spectrum. One obtains a measure free of aliasing from zero spatial frequency up to the sampling frequency.

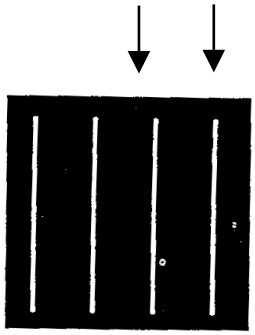

Fig. 2.8: View of a GLSF target

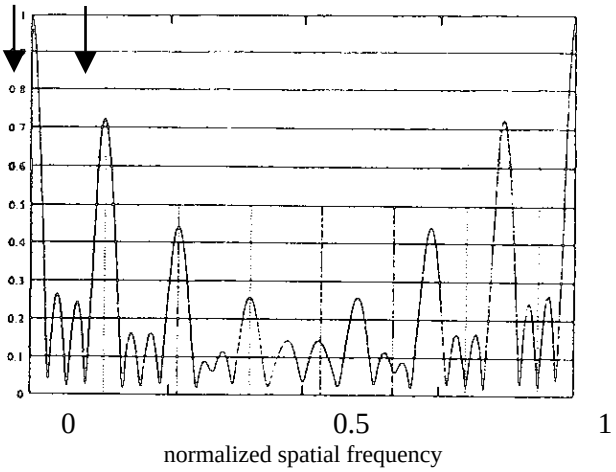

Fig. 2.9: Fourier spectrum of a GLSF target obtained at the output of a thermal imager. The spatial frequency is normalized with the sampling frequency. The arrows designate useful frequencies

The GLSF is the signal obtained perpendicular to the line pattern. Due to the periodicity of the test pattern and the choice of the distance between the lines, the Fourier transform of the GLSF at frequencies r_i, see Fig. 2.9, is not affected by the sampling of the imager and hence practically the same at different positions over the array.

2.7 FRACTAL TEST PATTERN TECHNIQUE

Two MTF assessment methods[10] have been designed which use large area grey-level test targets that are composed of a set of wavelet patterns distributed according to a fractal algorithm.

The first method uses a test target that has a random multiscale wavelet pattern distribution. It allows a statistical averaged measurement of the camera wavelet amplitude reduction according to the wavelet scale, thus providing a new figure of merit.

The second method consists in setting the measurement free from the aliasing effects. Its aim is to measure the system transfer response (base band) and the spurious response replicas (using the NVTherm keywords). This method uses a steady distribution of wavelet patterns and is based on the shape distortion analyse of the output wavelet patterns from the camera. The image processing analyse procedure is able to provide an automatic measurement technique without any mechanical adjustment requirements.

The feasibility of both methods was proved by using a computer simulation of a modelled camera measurement. However the main problem remains being the manufacturing of grey level test target.

2.7.1. Performance assessment with a random multi-element target

The test target for this first assessment method, Fig. 2.10, is composed of a set of wavelet patterns that are spatial frequency band limited. The patterns are distributed according to a fractal algorithm using random variables, in such a way that location of several pattern scales are randomly distributed on the target surface, without spatial overlapping between elements. Since the pattern cut-off frequency (Fw) is inversely proportional to the pattern scale, the several scale pattern set will provide a gradual evaluation of the aliasing phenomenon.

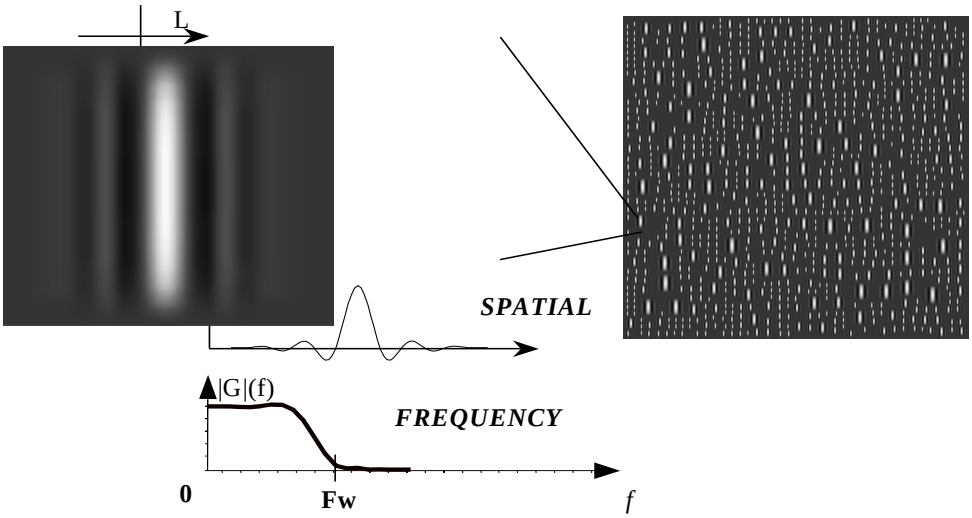

Fig. 2.10 Random multi-element target with band limited wavelet pattern (horizontal).

The statistical analysis of the camera wavelet amplitude reduction according to the wavelet scale gives a new figure of merit describing the average amplitude reduction yielded by aliasing and non perfect reconstruction of the camera (Fig. 2.11).

2.7.2. Performance assessment with a steady position multi-element target

The second resolution measurement method is based on steady position wavelet patterns with two pattern scales, Fig. 2.12. Large elements are dedicated to the small elements localisation in the image produced by the imager. The small elements responses are used for resolution assessment.

The calculation method uses some principles of the GLSF MTF measurement technique (see Section 2.6). It consists in finding the distortion periodicity number Kw of the small wavelet patterns aligned in columns, Fig. 2.13. The Kw extracted patterns horizontal luminance allows the calculation of a spectral representation of the sampling and reconstruction camera process. This figure of merit gives the system transfer response (pre-post filter response) and the spurious response replicas (post-filtered pre-filtered replicated responses). Fig. 2.14 shows an example of a simulated measurement, for an undersampled camera with a LED display, together with an image example.

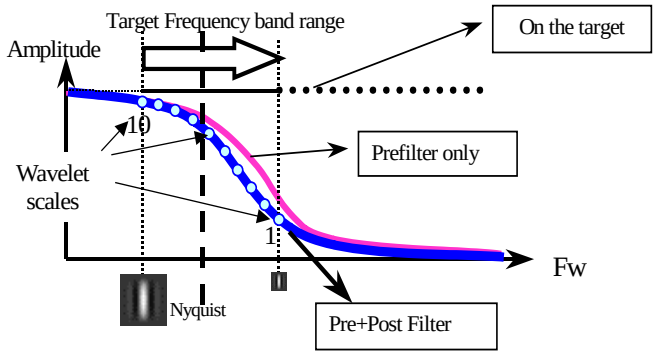

Fig. 2.11: Random multi-element target with band limited wavelet pattern (horizontal).

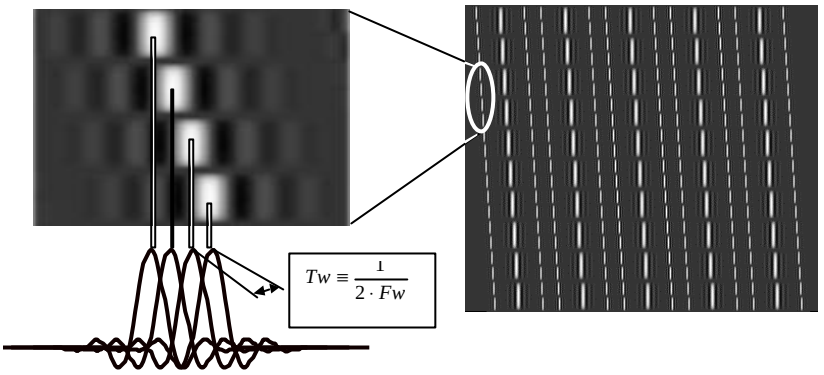

Fig. 2.12: Multi elements steady position target with band limited wavelet patterns (horizontal)

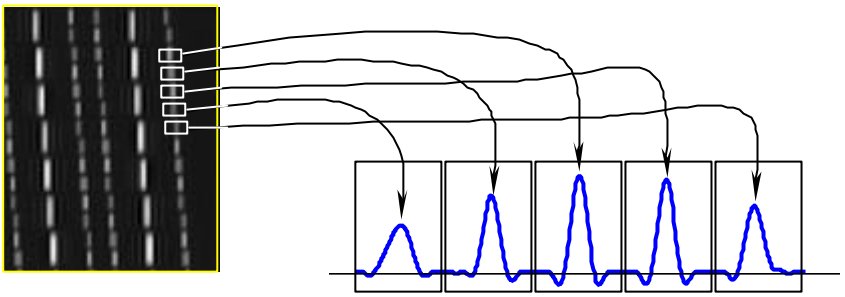

Fig. 2.13: Periodical wavelet distortion, and extraction of Kw patterns (here Kw=5).

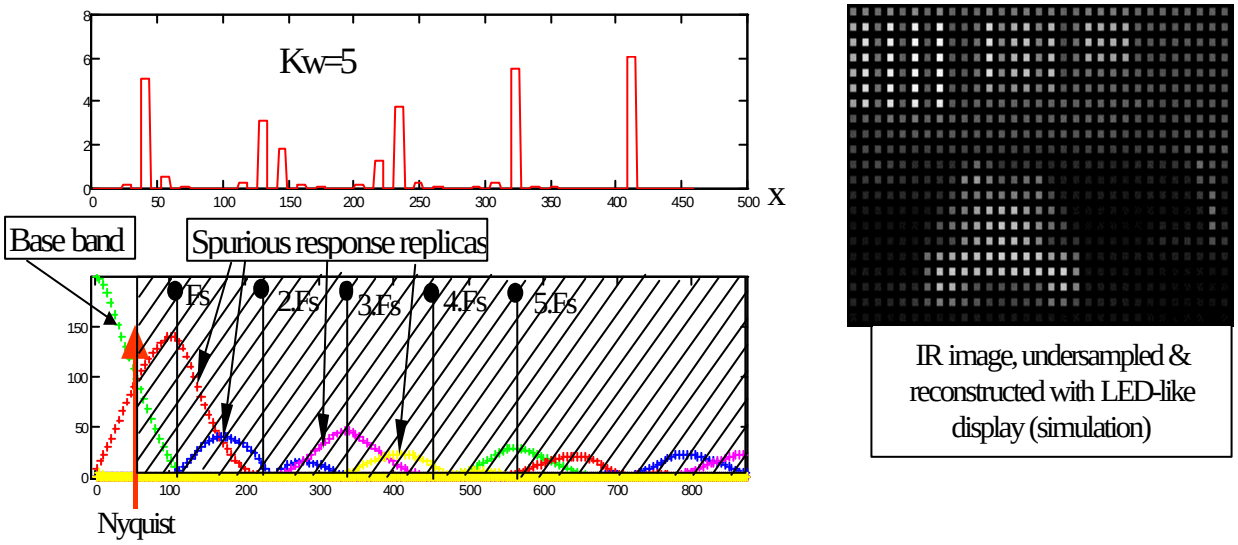

Fig. 2.14: System transfer response (base band) and the spurious response replicas.

2.8 AMOP

AMOP (Average Modulation at Optimum Phase) is a performance measure used in the TRM3 model. It is the average signal difference in the image of the 4-bar standard pattern, with the test pattern positioned at optimum phase. It can be measured in the video signal or on the display.

In case of well-sampled imagers, the signal difference between individual bars of the reconstructed test pattern is constant (assuming no noise) and independent of the position of the test pattern, see Fig. 2.15. (Classical performance models assume that this average signal is proportional to $4/\pi$ times the system MTF.)

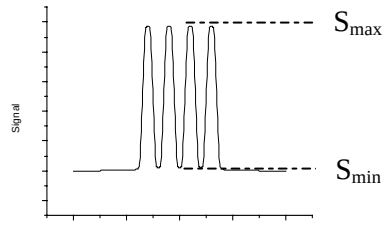

Fig. 2.15: Reconstructed signals of a standard 4-bar test pattern for a well-sampled low-pass filtered imager

For undersampled imagers the modulation between individual bars is not constant but depends on the position or phase of the test pattern relative to the detector matrix. An example is given in Fig. 2.16. With the nomenclature of Fig. 2.17, the average signal difference or 'bar strength' at phase φ is given by

$$\Delta S(r,\varphi) = \frac{1}{n-1} \cdot \sum_{i=1}^{n-1} \left| S_i - S_{i+1} \right|$$

It was shown that there is an optimum phase position at which the average signal difference is a maximum.[11] This average value is designated as AMOP.

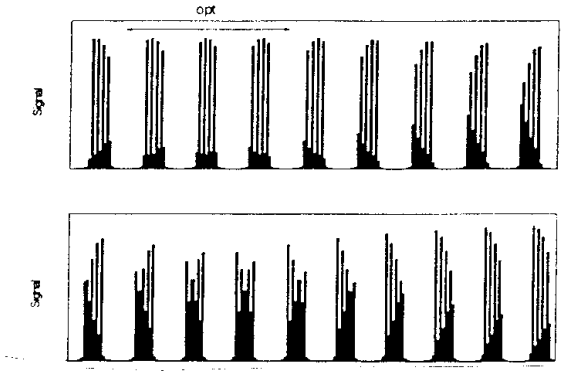

Fig. 2.16: Sampling of a 4-bar target having a spatial frequency near the Nyquist frequency and moving over a staring array. The reconstructed signal depends on the phase. The optimum phase is on the top right side of the figure.

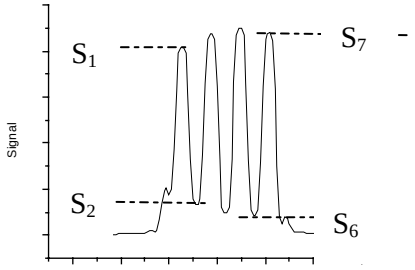

Fig. 2.17: Example of the signal variation in a sampled and reconstructed standard 4-bar target in case of an undersampled imager.

Fig. 2.18 gives an example of AMOP as function of spatial frequency, normalised with the sampling frequency. The prefilter MTF is also shown for comparison. AMOP takes values lower than $4/\pi$ times the prefilter MTF and drops to zero at about 0.9 times the sampling frequency of the imager. For details see the bibliography.

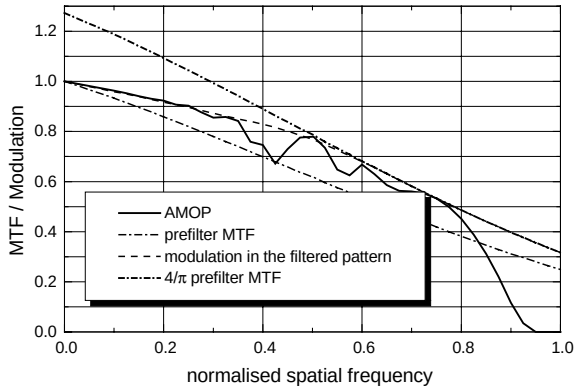

Fig. 2.18: Example of AMOP as function of the spatial frequency, normalized with the sampling frequency. AMOP takes values lower than $4/\pi$ times the prefilter MTF.

2.9 DOUBLE-SLIT METHOD

The double-slit method[12] uses two parallel line sources the distance of which can be varied. In general, the *modulation depth*, defined as the ratio of the signal dip v_d between both signal peaks and the peak signal v_m, is measured as function of the angular separations between the two line sources, see Fig. 2.19. The position (phase) of the double slit relative to the detector grid is optimised for maximum modulation depth.

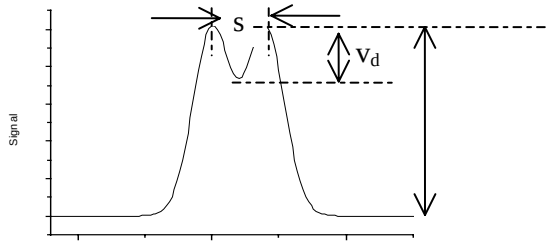

Fig. 2.19: Example of a signal obtained with the double-slit technique.

Fig. 2.20 shows the results of the measurements on the modulation depths, carried out on a number of cameras. One may observe the strong dependence of the modulation depth with the slit spacing.

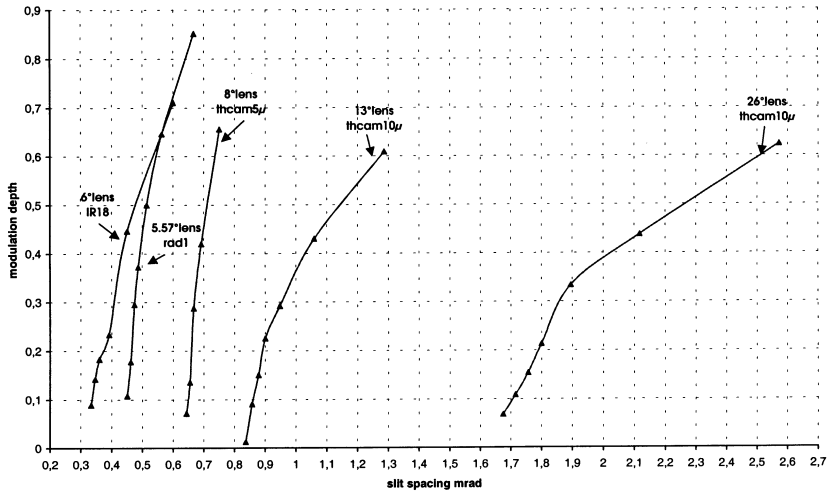

Fig. 2.20: Modulation depths measured with the double-slit technique.

The *resolution* in $mrad^{-1}$ is defined as the inverse distance for which the modulation depth is 10%. In general, the lines can be oriented in any direction: Measurements in the video signal are made for vertical double-slits where improvement of the signal to noise ratio is achieved by frame averaging. Measurements are obtained from the display with an external high-resolution video camera.

The advantage of the double-slit method is the ability to reach a fine adjustment of the focus and the definition of resolution similar to the classical Rayleigh criterion. The drawback is the non-direct relationship of the modulation depth with the classical MTF.

This page has been deliberately left blank

Page intentionnellement blanche

Chapter 3

Assessment of System Sensitivity

3.1 CLASSICAL FIGURES OF MERIT

Signal Transfer Function (SiTF) and Noise Equivalent Temperature Difference (NETD are the main figures of merit to assess dynamic range and thermal sensitivity of 1st generation scanning imagers.

The SiTF is the output signal (voltage or luminance) as function of the input signal (irradiance or temperature). This function is generally S-shaped with a linear region and saturation regions at low and high irradiances or temperatures. NETD is used to describe the temporal noise of the imager. It is defined as the temperature difference between an extended test target and the background that produces a signal equivalent to the temporal noise. The classical definition of NETD is referred to an electronic standard reference filter. It is measured in the analog output signal.

3.2 NOISE CHARACTERISATION OF ADVANCED SYSTEMS

Modern imaging sensors incorporating focal plane architectures have sophisticated post-detector processing and electronics. These advanced technical characteristics produces the generation of complex noise patterns in the output of the system. Unlike classical systems where “well-behaved” detector noise predominates, these complex systems have the ability to generate a wide variety of noise types each with distinctive characteristics temporally as well as along the vertical and horizontal image directions.

Such complex three-dimensional (time, vertical, horizontal) noise phenomena cannot be adequately treated by previous mathematical analyses developed for earlier simpler systems. Different techniques and assessment parameters were developed to characterise the noise in advanced systems. Also. detector elements with low responsivity, excessive noise or 1/f noise (*bad pixels*) must be identified, characterised and, if necessary, excluded from the measurements since they affect the measurement results.

3.2.1. General considerations

In advanced systems, noise measurements can be made at different output ports of the imager (digital or analog video) and in specified regions of interest. Generally, imager noise is assessed without using any filters. Bad pixels may or may not have been excluded from measurements. The results of noise measurements may strongly depend on the test conditions that must be reported when presenting data.

3.2.2. Temporal noise

Temporal noise can be assessed either separately for each detector by analysing the temporal variation of the detector signal, or as an average noise over many detectors. TG12 recommends using the term NETD only to characterise temporal noise. NETD should not be used for the joint assessment of spatial and temporal noise.

As already mentioned, temporal noise measurements shall not be performed with the classical standard reference filter or any other filter that limits the bandwidth of the video signal.

3.2.3. Spatial noise

Individual detector elements in infrared detector arrays have different photo response characteristics. Unless corrected, the displayed image is not uniform, even if a homogeneous scene at constant temperature is viewed: The detector non-uniformity appears as *stationary* or *fixed pattern noise in the*

image. Non-uniformity can vary with the type of technology, detector material and fabrication technique employed in the manufacture of a particular FPA as well as on post-detector processing and electronics.

High performance FPAs need to be able to resolve thermal image scenes with a temperature difference typically as small as 0.01 K, thus requiring the spatial non-uniformity to be in the same order of magnitude. Therefore, non-uniformity correction is a must.

3.2.4. Non-uniformity correction

The detector non-uniformity is corrected by measuring the detector signal responses at one, two or more uniform blackbody temperatures. The measured offset and (in case of a two-point correction) gain differences of each detector signal relative to the average offset and gain are used to calculate the required offset (and gain) correction. The correction is then applied to each detector signal with the aim to obtain uniform response.

The correction is never perfect, thus producing *residual non-uniformity* in the displayed image that needs to be assessed. Best correction is obtained at the calibration temperatures immediately after determining the correction coefficients. At other background temperatures the residual non-uniformity is higher. An example is shown in Fig. 3.1 for a system with two-point correction.

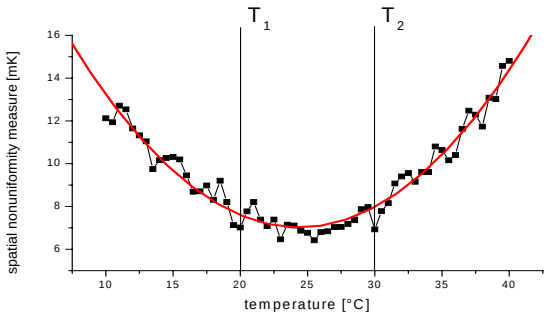

Fig 3.1: Measured spatial non-uniformity as function of the background temperature for an imager with two-point correction. (Calibration temperatures T_1 and T_2). Non-uniformity is not equal to zero at the calibration temperatures.

Residual non-uniformity also changes with time. This is due to the temporal instability of the detector elements in the array, which depends on detector type, detector manufacturing technology, cooler instability, etc.

3.2.5. Real-time non-uniformity correction

Real-time non-uniformity correction (NUC) methods serve to always keep the residual non-uniformity at a minimum level. The assessment of real-time NUC techniques is an important issue, which, however, was not addressed by TG12.

3.3 3-D NOISE MODEL

The 3-D noise model[13],[14] divides the total noise present into a set of eight components which have special properties related to temporal and spatial dimensions which form a three-dimensional coordinate system. One axis is time. The other two are horizontal and vertical dimension. When a number of frames are taken and recorded it is possible to obtain eight kind of data set, each of one corresponding to a different type of noise. These sets of data, N_x, are formed form the original set of frames by means of averaging operators.

The exact procedure to obtain these sets is complicate and too extensive to explain in this document, so the reader is invited to consult the bibliography.

N_{tvh}	Contains tvh noise
N_{vh}	Contains vh noise only
N_{th}	Contains th noise only
N_{tv}	Contains tv noise only
N_{v}	Contains v noise only
N_{h}	Contains h noise only
N_{t}	Contains t noise only

It is possible to obtain information about noise from this data set. For example, a figure of merit similar to IETD (see next paragraph) can be derived from the following expression,

$$\sigma_{vh} = std(N_{vh}(1-F))/R\,.$$

being F an operator that removes low frequency components from N_{vh} and "std" means standard deviation, R is the slope of the SiTF at measurement temperature. Similarly NETD can be compared with,

$$\sigma_{tvh} = std(N_{tvh}(1-F))/R\,.$$

Other noise descriptors can be defined in a similar way. The interest in this procedure is that it is similar to three factor components of a variance analysis in which temporal (frame-to-frame), vertical (row-to-row), and horizontal (column-to-column) effects are partitioned from the total noise present in the data set. It permits a characterization of different kinds of noise what will be important in follow sections (MRTD, MTDP). It is valid, too, for scanning and staring systems. For scanning systems with analog output it is necessary to digitise the image before applying the method.

3.4 IETD

The IETD[15] (Inhomogeneity Equivalent Temperature Difference) describes the RMS-variation of *randomly* distributed fixed pattern noise in terms of temperature, similar to NETD, which describes the temporal high frequency noise of the imager.

IETD is defined as:

$$IETD(T) = \frac{\sigma_V}{dV/dT}\,.$$

where σ_V is the RMS value of the randomly distributed fixed pattern noise voltage and dV/dT is the responsivity of the system.

To calculate IETD, low frequency contributions and periodic artefacts (stationary or pseudo-stationary line or column structures) are removed by high-pass filtering and clipping of excessive frequency components from the measured fixed pattern noise signal. An example is given in Fig. 3.2

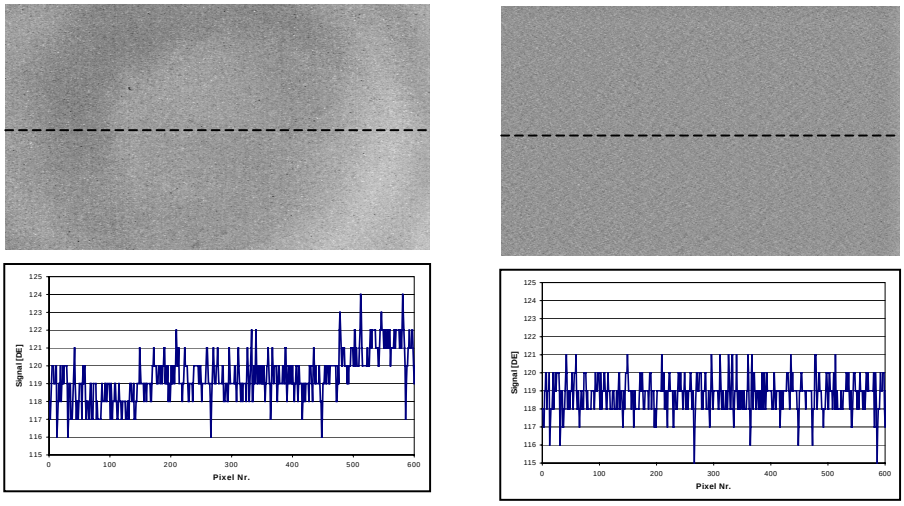

Fig 3.2: Thermal image after two-point correction (top left) and signal variation in a horizontal line (bottom left). The same image after high-pass filtering (top right) and line signal after high-pass filtering (bottom right).

The actual fixed pattern noise in an advanced imager may be more complex due to spatial and spatial-temporal artefacts introduced by imperfect electronic circuits (periodic or pseudo-periodic line patterns, low frequency variations, flicker, etc). IETD assesses only that contribution of spatial and temporal-temporal noise whose impact on system performance can be modelled analytically.

3.5 CORRECTABILITY

This figure of merit[16] provides an estimate of the residual spatial noise after calibration correction of the camera, relative to the temporal noise. A correctability value of one means that spatial noise after correction is equal to temporal noise. A value smaller than one means that spatial noise is lower than temporal noise.

The correctability figure of merit is based on the statistical analysis of noise data taken at various background temperatures. The statistics is described as follows

$$\chi_j^2 = \sum_{i=1}^{n} \frac{\left(y_{ij}^c - < y_i >\right)^2}{y_{ti}^2} \quad ,$$

where y_{ij}^c is the value of the pixel j after correction at temperature i , $\langle y_i \rangle$ the mean signal of the array at temperature i and y_{ti} the temporal noise of the array at temperature i. The χ^2 distribution for a FPA with uniform response and randomly distributed Gaussian temporal noise is well known in statistics.

Deviations of the measured χ^2 histogram from the ideal distribution, see Fig. 3.3, are due to the residual spatial non-uniformity in the array. After subtracting the ideal distribution due to temporal noise from the real distribution after correction, one obtains a measure to estimate the quality of the array. This measure is defined the *correctability* of the focal plane array. It is given by

$$c = \sqrt{\frac{\sum_{j=1}^{N} \chi_j^2}{(N-1)(n-r)} - 1} = \sqrt{\frac{\sum_{j=1}^{N} \sum_{i=1}^{n} \frac{(y_{ij}^c - < y_i >)^2}{y_{ti}^2}}{(N-1)(n-r)} - 1} \quad ,$$

where N is the number of pixels in each frame of data taken,

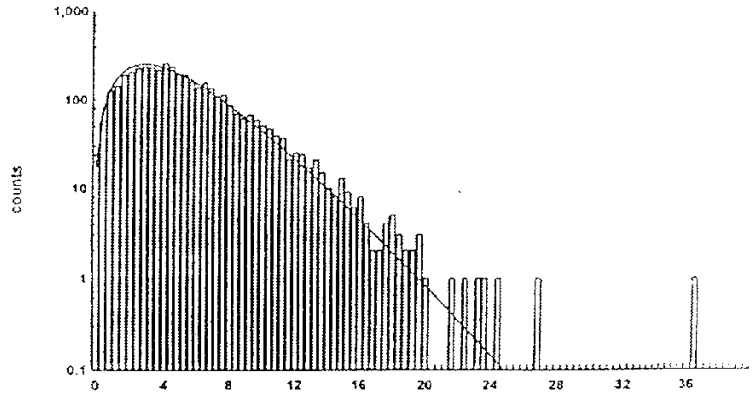

Fig 3.3: Probability Distribution Histogram and theoretical distribution.

3.6 THE PRINCIPAL COMPONENT APPROACH

A different approach of characterizing thermal imager noise is by performing a principal component decomposition.[17] Its general objectives are data reduction and interpretation of noise data.

The set of noisy frames provided by a thermal imager with M detectors is represented as an N x M matrix F with

$$F = \{F_1, F_2, \ldots, F_t, \ldots\ldots F_N,\} \ ,$$

where N is the number of frames and F_t is the frame taken at a given time. F contains the full set of data to be analysed. Each frame can be considered a random variable. The realisations of this variable are the signals obtained by each detector at the given frame. To demonstrate the approach, Fig. 3.4 gives an example with three frames.

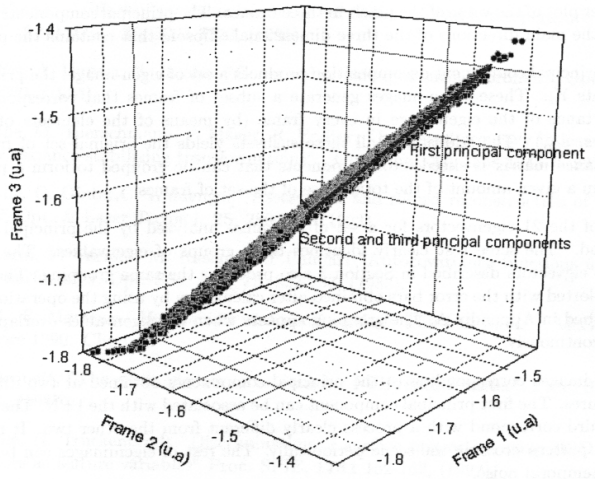

Fig 3.4: Scatter plot of the pixel values in the three frames indicating the principal components

Each detector is represented as a point whose coordinates are the three different signal values of that detector in the three frames. When all the pixels are located in this diagram a cloud of dots is obtained. In Fig. 3.4 the pixels are mainly aligned along a given direction. This direction corresponds to the first

principal component which contributes most to the variance of the data. The second and third principal components are located in planes perpendicular to the first one.

The principal component decomposition takes this set of image frames as a linear combination of eigen-images, each one associated with one principal component, see Fig. 3.5. When applying the method to the analysis of noisy images, it allows to identify the different noise processes involved in the noise and to calculate the contribution of these noise processes to the total noise variance.

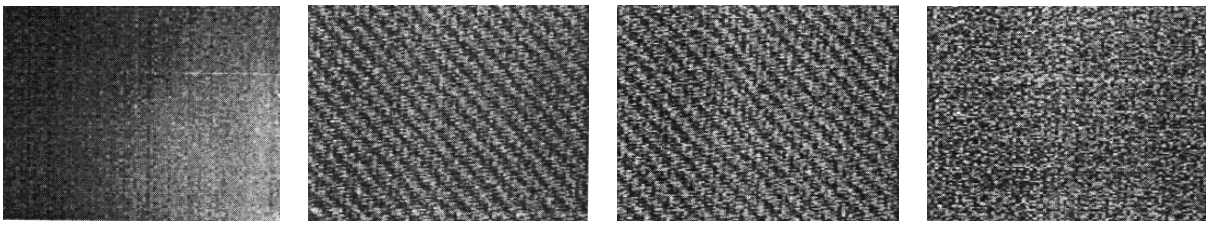

Fig 3.5: Eigen-images of the first four principal components in a set of noise frames. The first eigen-image is associated with stationary fixed pattern noise. The second and third eigen-image is associated with a fringe pattern crossing the scene periodically. The fourth is associated with temporal noise.

The correlation coefficients defined by Mooney[18] can be calculated by means of the covariance matrix for the different noise processes. Also, the 3-D methodology can be applied to each noise process separately. The results of the method can be presented as images. Therefore, the analysis of spatial patterns associated with each type of noise process is easily derived. The technique allows a very detailed assessment of the imager noise, which cannot be accomplished by previous methods.

3.7 BAD PIXEL CHARACTERIZATION

3.7.1. Phenomenology and definitions

RSG16 of NATO/AC243 adopted the following definitions.[19]

- *Bad pixel:* Those detector elements (pixels) in a focal plane array which are either permanently dead or which show abnormal characteristics are called bad pixels.
- *Dead pixel:* *A* detector element is a dead pixel if it has no response at all; i.e.

$$R_i = \frac{\Delta S_i(T)}{\Delta T} = 0$$

- *Abnormal pixel:* A detector element is defined as abnormal if one of the two following conditions are met:
  - excessive temporal noise, i.e. NETD > $NETD_{tolerable}$
  - correctability is above a specified threshold

Abnormal pixels have one or several of the following features:

- Excessive temporal noise
- Detector response beyond tolerable limits
- Detector offset beyond tolerable limits
- Unacceptable temporal signal variations (1/f noise; deviant flashers; blinker)

The general assessment of bad pixels is addressed in the next two paragraphs. The assessment of unacceptable temporal signal variations is treated in Sections 3.74 and 3.75.

3.7.2. Bad pixel assessment with the correctability concept

The correctability concept can be used to characterize any abnormal feature of a pixel, except for excessive noise. A pixel can be characterized as a bad pixel if its χ_j^2 value exceeds the value at which the ideal χ^2 distribution of only temporal noise is zero (see Fig. 3.3). The concept permits to specify a reasonable threshold to eliminate bad pixels in a focal plane.

The correlation between bad pixels as defined by an excessive NETD and by the correctability procedure was investigated.[20]

3.7.3. Bad pixel assessment with the principal component approach

It is possible to define an *average or mean pixel* as a pixel that exhibits the mean behaviour with respect to the principal components. Its components are the mean components of all pixels with respect to each principal component. A distance measure is introduced to characterise the distance between each individual pixel and the mean or average pixel.[21] This is illustrated in Fig. 3.6. Different distances measures can be introduced depending on the required data analysis.

A detector element is considered being a bad pixel if its distance from the average pixel exceeds a specified threshold value.

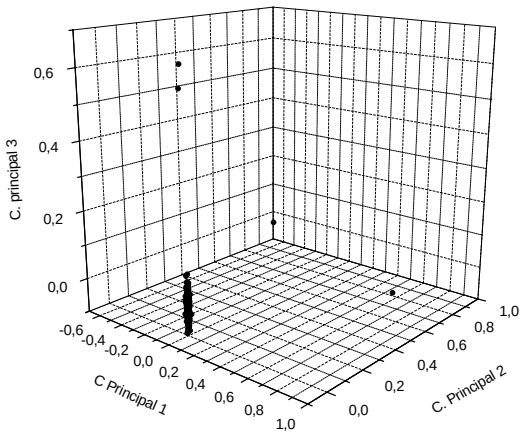

Fig. 3.6: View of the detectors in the principal component coordinate system. Some pixels can easily be identified as bad pixels.

3.7.4. 1/f noise, long term stability

Detector elements with unacceptable temporal signal behaviour, see Fig. 3.7, were designated[22] as either

- Weak *pixel:* Detector elements showing a weak sensitivity. The corrections procedure strongly amplifies the noise together with the signal
- *Blinker pixels*: Detector elements characterized by a burst noise switching between two or more states. They give a high contribution to the 1/f noise
- *Drifting pixels*: Elements who exhibit a slow drift of its mean signal value. They also give a great contribution to the 1/f noise.

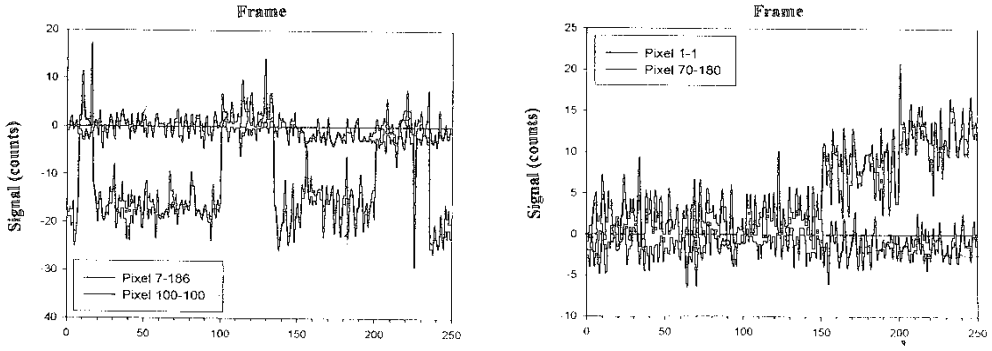

Fig 3.7: Temporal signal variations of a *blinker pixel* (left) and of a *drifting pixel* (right). For comparison, the temporal signal variation of a regular detector element is also shown in the two graphs.

Unacceptable temporal signal behaviour is characterized as 1/f noise. 1/f noise is present in many of FPA imagers. It is detected by analysing the noise power spectrum of individual detector elements. The 1/f slope in the spectrum can easily be identified in a log-log plot. Normally, this kind of noise enhances low temporal frequencies compared to high temporal frequencies. It represents a low frequency trend in the detector signal. To detect and measure 1/f noise it is necessary to record frames during long periods of time (normally minutes and hours). Fig. 3.8 shows as an example the signal of a detector with 1/f noise and its noise power spectrum.

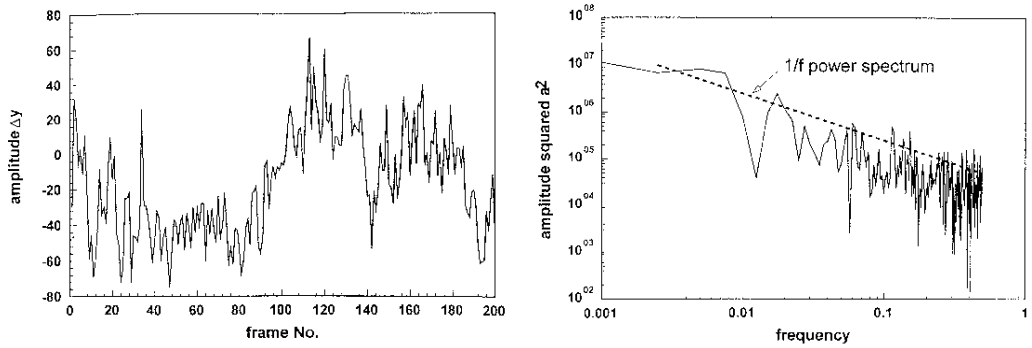

Fig 3.8: Typical signal variation in a detector element with 1/f noise (left) and associated noise power spectrum (right). Units are arbitrary.

3.7.5. 1/f noise assessment with the correctability

The correctability approach allows the assessment of 1/f noise[23]. 1/f noise affects correctability in two ways:

- The maximum of the χ^2 histogram is moved toward lower values.
- The tail of the χ^2 histogram becomes longer; an indicator for a large number of non-correctable pixels.

From the χ^2 histogram the 1/f coefficient, c_f, is derived which is given by

$$c_f = (\sigma_{ms}^2 - \sigma_{mx}^2) / \sigma_{mx}^2$$

where

$$\sigma_{mx}^2 = \frac{\chi_{\max}^2}{n-3} \quad \text{and} \quad \sigma_{ms}^2 = \frac{<\chi^2>}{n-1}$$

n is the number of frames used for the analysis of the correctability, χ_{max}^2 the maximum χ^2 value and $<\chi^2>$ the mean square of the histogram. If the arrays has no pixels with 1/f noise c_f is zero. In the presence of 1/f noise the histogram is deformed and c_f increases with the "amount" of 1/f noise present.

This page has been deliberately left blank

Page intentionnellement blanche

Chapter 4

Overall Performance Measures

4.1 INTRODUCTION

The figures of merit outlined in previous sections characterize the imager in terms of resolution and sensitivity. In this section overall device performance characterization is addressed.

Figures of merit that assess the overall device performance must include the thermal sensitivity of the imager, its spatial resolution including the sampling of information, and observer performance. The classical MRTD, which is shortly reviewed in the next paragraph, is not suited to assess undersampled advanced imagers. New techniques were developed which are described in the remaining sections of this section.

Human observers determine the figures of merit described in Sections 4.2 to 4.6. The results obtained with these measures are of subjective nature. Several objective techniques were developed that are described in Sections 4.7 and 4.8. These techniques replace the human observer by an eye-brain model.

4.1.1. MRTD and undersampling

MRTD (Minimum Resolvable Temperature Difference) is the classical figure of merit developed for 1st generation imagers. It is the minimum temperature difference at which the four bars of the standard 4-bar test pattern are resolved by an observer. The measurement procedure is standardized in STANAG 4349.24

If the imager is undersampled, the image of the 4-bar test pattern depends on the position of the test pattern relative to the detector array (phase). The four bars can be resolved only at pattern frequencies lower than about 0.55 times the sampling frequency. At higher frequencies the four bars cannot be resolved due to aliasing. This is illustrated in Fig. 4.1.

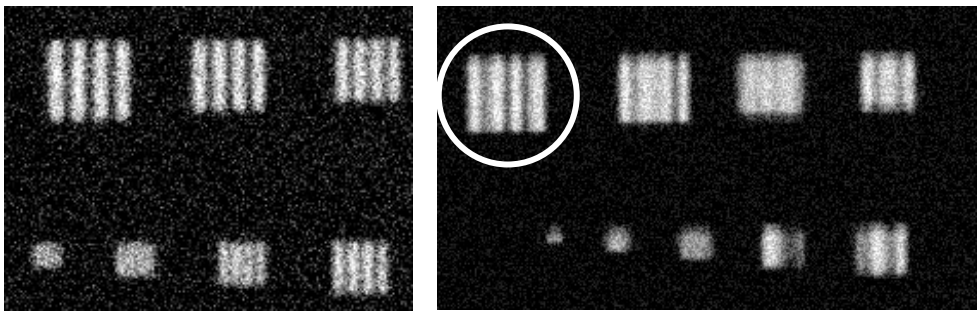

Fig. 4.1: Images of standard 4-bar test patterns obtained with a well-sampled imager (left) and an undersampled one (right).

If undersampled, the four bars can be perceived only at pattern frequencies lower than approximately the Nyquist frequency. Shape and modulation of the displayed bar pattern depends on the phase (see the encircled pattern). At frequencies greater than the Nyquist frequency the four bars cannot be resolved.

4.2 STATIC MRTD

Figure 4.2 shows the static approach to measuring MRT of a staring sensor. At each frequency or bar pattern, the phase is found which optimises the MRT. To vary the phase, the target wheel is placed on a translating stage, or, equivalently, the sensor is placed on a motorized rotational stage. The phase is considered the angular target position with respect to the sensor detector. While the observer views the 4-bar target, the stage is adjusted (i.e. the phase is varied) or the sensor is micro-positioned to peak up the 4-bar target modulation. Between 0.6 and 0.9 times the half-sample rate of the sensor, it is extremely difficult to ensure that correct target phase is accomplished. The results vary greatly with phase and from observer to observer. Figure 4.2 on the right side shows two images of a 4-bar target where one target is positioned at best phase and the other target is positioned at worst phase. Figure 4.3 shows the MRT for a sensor at best phase and at worst phase. Also note in the static MRT Figure, the MRT is measured past the half-sample rate of the sensor for the best phase case. [25]

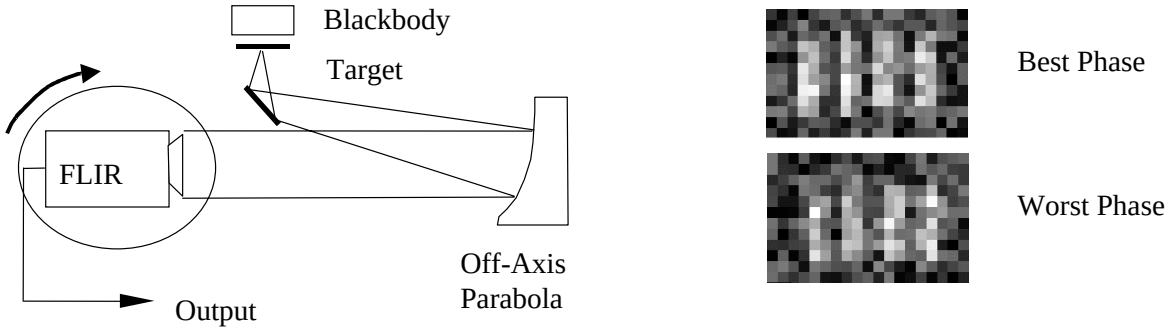

Fig. 4.2: Sample imaging system MRTD test configuration (left) and images of the standard 4-bar target at best and worst phase (right).

4.3 DYNAMIC MRTD

In order to address the phase and sampling problems associated with the MRT measurement, Webb [26] developed the dynamic MRT measurement where the MRT target is moved across the sensor field of view during the MRT measurement. The technique is known as the Dynamic MRT (DMRT) and the MRT is measured as the target is moved through the sensor's field-of-view.

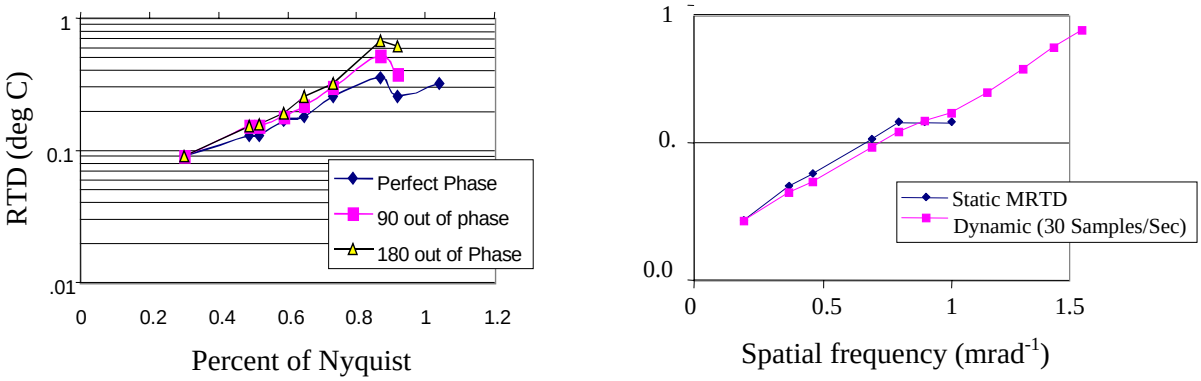

Fig. 4.3: Static MRTD measurements at different phases (left) and comparison of static and dynamic MRTD measurements (right).

It has been shown that the DMRT can measure system performance up to the MTF limit of the system and eliminates the problems associated with static sampling and phase optimisation. The increase in MRT performance is measured due to an increase in the sample rate across the target (as the target moves across the sampling grid).

There are two characteristics here worth mentioning. First, while the sampling effect has been minimized in the DMRT measurement, there has been an additional MTF blur introduced by the motion of the target. The DMRT measurement changes with target velocity through the sensor field-of-view since both the spatial sampling rate has changed and the blur due to motion has changed. The DMRT measurement beyond the half-sample rate of the sensor is useful and can be modified for use in acquisition calculations. Webb and Halford describe the DMRT method in detail. [27]

4.4 MTDP

The MTDP[28] (Minimum Temperature Difference Perceived) allows assessment of both well-sampled and undersampled imagers. The MTDP figure of merit is used in the German TRM3 model. It is based on the perception of the standard 4-bar test pattern. The MTDP concept accepts that in case of undersampling the image of the standard test pattern is distorted and that less than four bars are resolvable at pattern frequencies greater than about half the sampling frequency.

MTDP is defined as the minimum temperature difference at which the four, three or two bars of the (distorted) test pattern are resolved by an observer. It is defined for and measured at *optimum phase* (see Section 2.8). For a well-sampled imager each phase is optimum and hence MTDP and MRTD become the same.

To measure MTDP, first the optimum phase has to be found at a sufficiently high ΔT. Once the pattern is positioned at optimum phase, the same procedures are used as in MRTD measurements. MTDP is related with AMOP (see Section 2.8) as follows:

$$MTDP(r) = \frac{\pi / 2 \cdot SNR_{thr} \Psi^{1/2}(r)}{AMOP(r)}$$

where SNR_{thr} is a threshold signal-noise-ration and Ψ a noise term. MTDP measurements can be made up to spatial frequencies of approximately 1.8 times the Nyquist frequency. The limiting frequency depends on the amount of undersampling, see Fig. 4.4. In Fig. 4.5 a measured MTDP is shown and compared with the prediction made with TRM3.

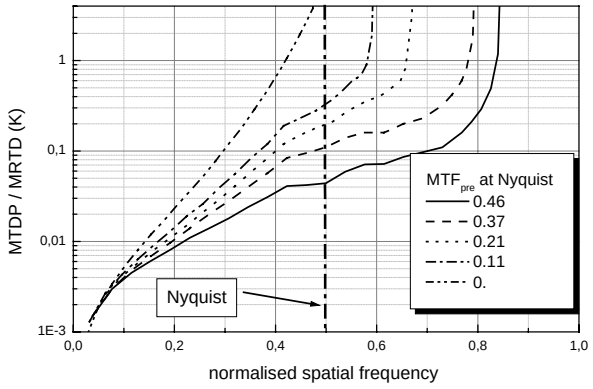

Fig. 4.4: MTDP and sampling. MTDP as function of spatial frequency normalized with the sampling frequency. Undersampling is characterized by the prefilter MTF at Nyquist. For a well-sampled imager (MTF at Nyquist = 0), MTDP and MRTD are the same.

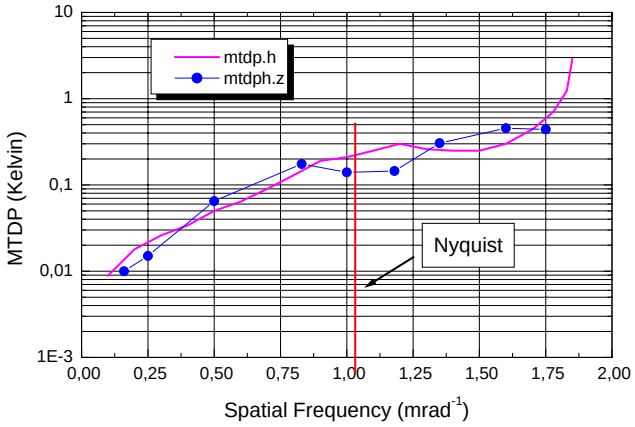

Fig. 4.5: Example of a measured MTDP (circles) and comparison with its prediction by TRM3

4.5 TOD (TRIANGLE ORIENTATION DISCRIMINATION THRESHOLD)

Another approach is the TOD (Triangle Orientation Discrimination threshold) methodology. [29,30] The TOD deals with the half-sample rate limit problem associated with the MRT/FLIR92 method by using an alternative, *non-periodic* test pattern: an equilateral triangle in four possible orientations (apex Up, Down, Left or Right, see Fig. 4.6, panel A).

At the same time, the laboratory measurement uses a robust 4AFC (Four Alternative Forced-Choice) psychophysical procedure instead of the subjective MRT measurement procedure. In this procedure, the observer has to indicate which triangle orientation he sees, even if he is not sure. Variation of triangle contrast and/or size leads to a variation in the percentage correct between 25% (complete guess) and 100%, and by interpolation the exact 75% correct threshold can be obtained (see panel B). A complete TOD curve (comparable to an MRT curve) is obtained by plotting the contrast thresholds as a function of the reciprocal of the triangle angular size (see panel C). A detailed description of the measurement of a TOD curve is given in [30].

The TOD method has a large number of theoretical and practical advantages: it is suitable for under-sampled and well-sampled electro-optical and optical imaging systems in both the thermal and visual domains, it has a close relationship to real target acquisition, and the observer task is easy. The results are free from observer bias and allow statistical significance tests. The laboratory method may be implemented in current MRT test equipment with little effort, and the TOD curve can be used easily in a TA model such as ACQUIRE. In addition, the method lends itself very well for automatic measurement using a human observer model.[31,32]

Three validation studies with real targets, including the simulation experiment described in the NATO TG.12 Topic 1 Final Report, show that the TOD curve predicts TA performance for under-sampled and well-sampled imaging systems very well. Currently, a theoretical sensor model to predict the TOD (comparable to NVTherm or TRM3) is under development.

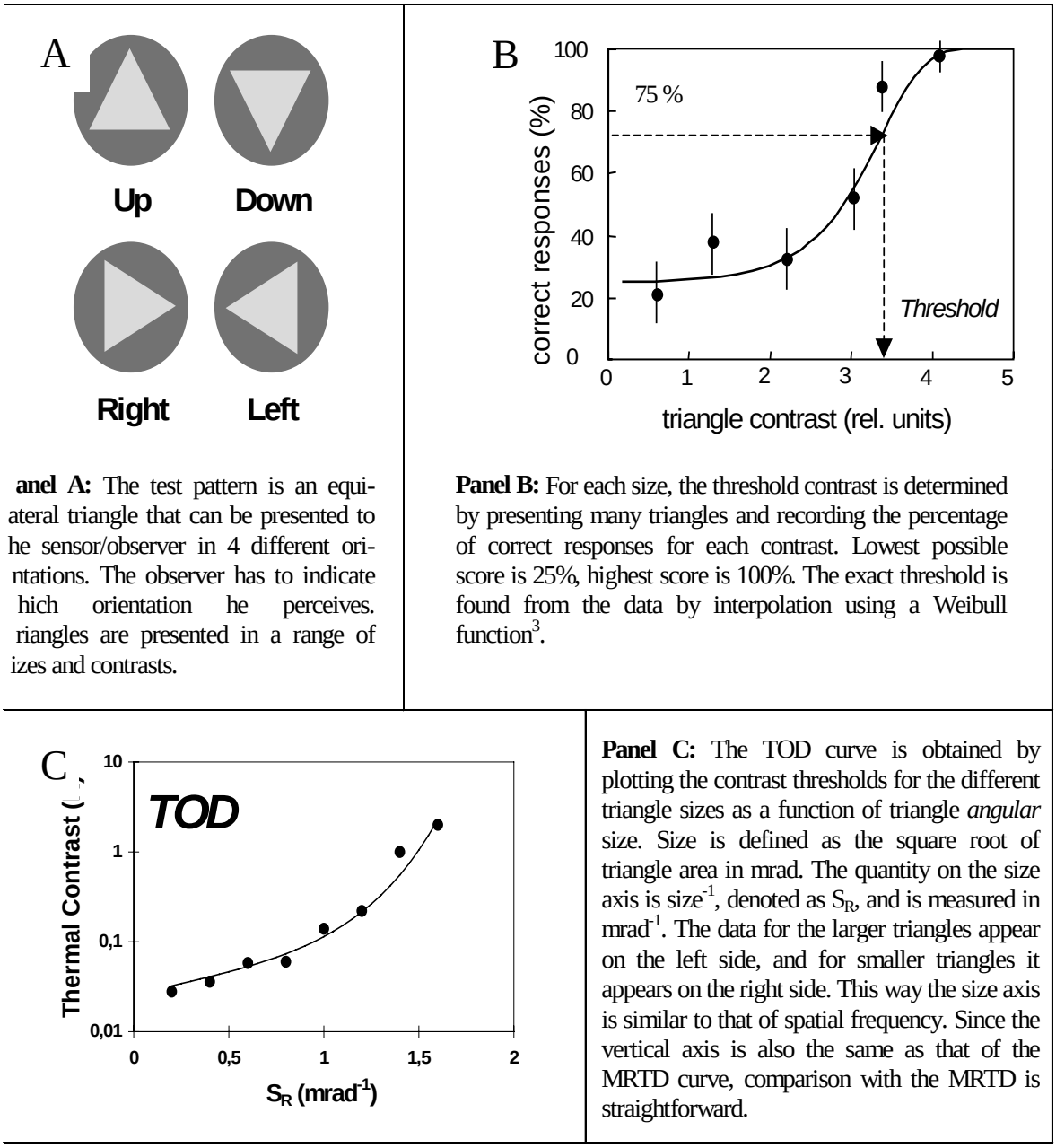

anel A: The test pattern is an equi-ateral triangle that can be presented to he sensor/observer in 4 different ori-ntations. The observer has to indicate hich orientation he perceives. riangles are presented in a range of izes and contrasts.

Panel B: For each size, the threshold contrast is determined by presenting many triangles and recording the percentage of correct responses for each contrast. Lowest possible score is 25%, highest score is 100%. The exact threshold is found from the data by interpolation using a Weibull function[3].

Panel C: The TOD curve is obtained by plotting the contrast thresholds for the different triangle sizes as a function of triangle *angular* size. Size is defined as the square root of triangle area in mrad. The quantity on the size axis is size^{-1}, denoted as S_R, and is measured in mrad^{-1}. The data for the larger triangles appear on the left side, and for smaller triangles it appears on the right side. This way the size axis is similar to that of spatial frequency. Since the vertical axis is also the same as that of the MRTD curve, comparison with the MRTD is straightforward.

Fig 4.6: The TOD method in a nut shell

4.6 MRID

This MRID figure of merit (Minimum Resolvable Intensity Difference) uses two parallel line sources with variable distance as test pattern. The observer is looking to a display and notes the minimum distance between the two lines, at which he can just discriminate them as two lines. This is analog to the classical Rayleigh criterion that refers to a point source rather than a line source. The MRID is then defined as the intensity difference of the two lines for a given line separation distance, required by the observer to be able to discriminate the two lines. Rather than the spatial frequency, the inverse of the separation distance is given as spatial parameter.

There are a number of benefits for this type of double-line targets such as

- the slit distance is easy to vary, so in the spatial domain one does not need a large number of bar patterns
- line sources are easy to model; they do not have higher harmonics like the bars
- modulation depth is strongly dependent on the slit separation distance
- the use of two lines excludes the wrong number counting as is the case with the 4 bars, where one may observe 2 or 3 bars beyond the Nyquist frequency
- the double-slit method can be used for objective as well as subjective performance measurements
- the target is easy to manufacture and cheap

An example of imagery of double line sources is shown in Fig. 4.7 for two slit distances. In the picture on the left side the two slits are just discernable. For more details see ref. [12].

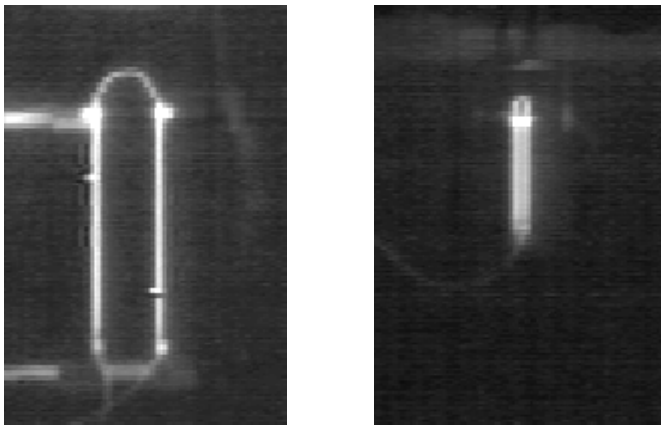

Fig 4.7: Images of the double slit test pattern at two different slit distances. In the picture on the right side the two slits are just discernable

Similar to the MRTD curve described before, one can define an *MRID* curve where the intensity is specified for the line source. The apparent intensity of the wire is calibrated with an extended blackbody source, covering an area containing several detector-elements. MRID can be used to predict the range performance of thermal imagers similar to the approach of STANAG 4347.

A comparison of MRTD (limited at Nyquist), MTDP and MRID is shown in Fig. 4.8.

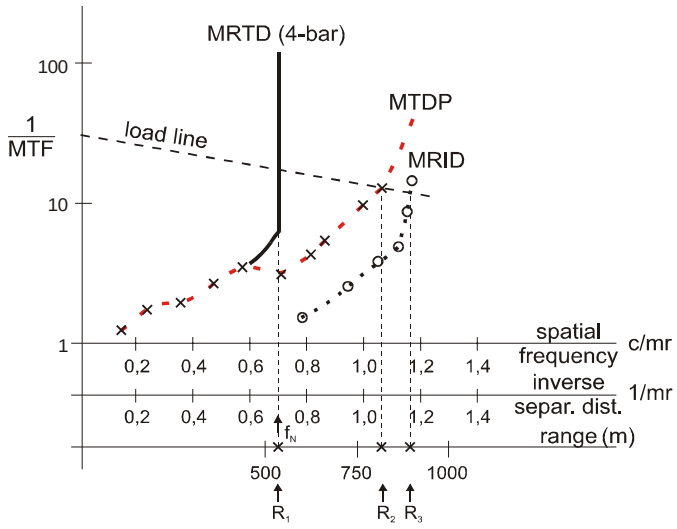

Fig 4.8: Comparison of MRID with MTDP and MRTD limited at Nyquist.

4.7 MRTD DERIVED FROM LSF AND NOISE MEASUREMENTS

This 'objective' technique[33] is utilizing a target set-up as shown in Fig. 4.9 with two-tilted line sources and an area source with a fixed temperature difference ΔT to its background. The camera under test is focussed to the two-line sources L_1 and L_2 by measuring the video signal of the thermal imager and maximizing this signal. A high-resolution video camera is used to image the display of the imager under test in such a way that only part (e.g. 1/3) of the field of view is covered in order to obtain sufficient oversampling. The gain setting of both the imager under test and the video camera is set in such a way that the signal of the extended area source as well as the line sources stay within the linear region of the Signal Transfer function. If necessary their temperatures are reset to appropriate values.

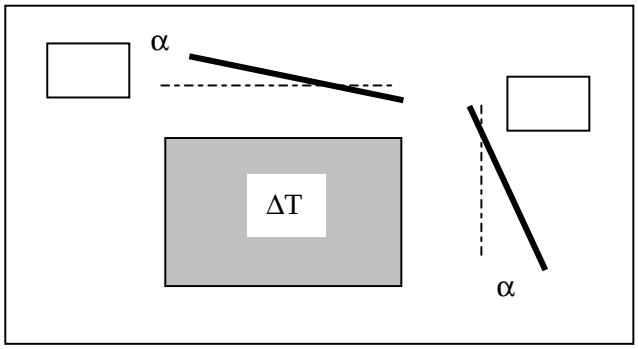

Fig 4.9: Target used in LSF + Noise Objective MRTD method. Two lines sources tilted by an angle α and an extended blackbody source.

The noise is measured from the video output as RMS value of the signal bit levels in the extended target area. By taking the responsivity the NETD is calculated. Horizontal and vertical MTFs are calculated from the Left's for line sources L_1 and L_2. Finally, the MRTD is obtained by using the empirical formula:

$$MRTD_{calc}(r) = \frac{c \cdot NETD \cdot FF_e}{MTF(r) \cdot MTF_e(r)}$$

where $FF_e(r)$ and $MTF_e(r)$ are the eye filter function and the eye MTF; c is a constant determined by comparison of $MRTD_{calc}(r)$ with a subjectively measured MRTD.

4.8 MATCHED FILTER TECHNIQUE

This technique assumes that the eye-brain channel acts like a matched filter in order to perceive a signal buried in noise. The signal is perceived if the signal-noise ratio at the output of the matched filter exceeds a threshold. These assumptions are the same as in most analytical performance models.

The matched filter approach applied to the perception of the displayed 4-bar pattern images assumes that the signal-noise ratio at the output of the matched filter is proportional to the MRTD or MTDP of the sensor. The technique consists in constructing the matched filter which is then used to filter the displayed images of the 4-bar pattern.[34]

To obtain the matched filter, images of the 4-bar test pattern are recorded for each pattern frequency at high temperature differences. If necessary, several frames are averaged to further minimize the noise. One dimension (1D) and two dimension (2D) match filters can be constructed. The filter is then applied to a series of low contrast images that are obtained over a range of small temperature differences, where the actual range of temperature differences depends on the sensor under test. In addition to the low contrast

bar patterns, images of an open position on the filter wheel are also acquired at each temperature. These images are used to determine the noise.

Algorithm MRTD and MTDP values are compared to subjective values obtained by human observers in Fig. 4.10. MRTD values were calculated based on matched filters corresponding to the pattern (corrected reconstructed) and its derivative (corrected difference). The results of the corrected difference are in good agreement with the subjective values, but more research is required to validate this approach.

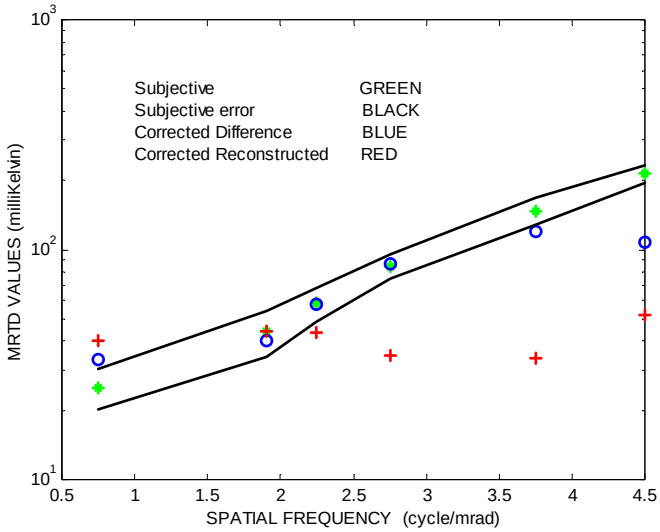

Fig. 4.10: Subjective (open circles) and corrected difference (solid circles) and reconstructed (crosses) MRTD values are compared. The agreement between the difference and subjective values is quite good.

Chapter 5

Discussion

A variety of measures and measurement techniques have been developed or evaluated to characterise the performance of advanced thermal imagers with respect to their

- geometrical (spatial) resolution
- thermal resolution (responsivity and noise)
- overall device performance characterisation.

In addition to the new overall device performance figures of merit which depend on the subjective assessment by a human observer, alternative "objectives" techniques have been developed and discussed. Performance measures developed for 1st generation thermal imagers which can also be used without modifications for advanced systems were not addressed.

5.1 GEOMETRICAL RESOLUTION

Measures and techniques developed or investigated to characterise the geometrical resolution are summarised in Tabel 5.1. The following techniques appear to be of special interest: The scanning slit method is the most accurate technique. It can be used to assess the system in any direction and can be applied to perform measurements in the digital and analog video signals as well as from the display. The double slit technique is a measure of the minimum distance at which the modulation depth reaches a certain value. AMOP is an overall resolution measure that is directly linked to the standard 4-bar technique.

Technique	Advantages	Disadvantages
Best, worst 'MTF'	fast; simple assessement of undersampling	no information on MTF
Scanning Slit	very accurate not affected by spatial noise	
Tilted Slit		low number of data correction of spatial noise
Discrete MTF	elegant	digital video output only correction of spatial noise
Double Slit	similar to Rayleigh criterion	no information on MTF special test pattern
Generalized LSF		special test pattern low number of MTF data
Fractal technique		complicated test patterns
AMOP	overall performance measure incl. undersampling	setting of optimum phase

Table 5.1: Measures and techniques for determining the geometrical resolution of advanced thermal imagers

5.2 THERMAL RESOLUTION

Proposed and investigated measures and techniques to assess thermal resolution are summarised in Table 5.2

NETD and *IETD* are simple measures characterizing temporal and random fixed pattern noise but, presently, a standardized definition of these terms is missing. With the *3-D noise* and the *principle components* techniques all possible noise terms in thermal imagers can be characterised. The principle components technique appears to be the most promising since it allows to identify the noise sources in the imager. The characterization of *bad pixels* and of *1/f noise* is an important aspect in assessing thermal imager noise for which special assessment techniques are now available.

Technique	Advantages	Disadvantages
NETD	input to performance models	different definitions exist
IETD	input to performance models	not standardized
3 D Noise	full noise characterisation	complex mathematical analysis
Schultz	basis for bad pixel and 1/f noise assessment	
Principle components	identifies principal noise contributions in the imager	complex mathematical analysis
Bad pixel and 1/f noise characterisation	quantitative basis for detector specification	

Table 5.2: Measures and techniques for determining the thermal resolution of advanced thermal imagers

5.3 OVERALL DEVICE PERFORMANCE

Subjective overall device performance figures of merit are summarised in Table 5.3.

Technique	Advantages	Disadvantages
Dynamic MRTD	uses classical resolution criterion	not related to other performance measures
MTDP	evolution of the MRTD concept; can be predicted and is input for range performance modelling	
TOD	less subjective due to forced choice method	no standard 4-bar test pattern;
MRID	resolution defined similar to the Rayleigh criterion	still in its infancy; relation with range performance not yet shown

Table 5.3: Figures of merit and techniques for determining the overall device performance of advanced thermal imagers

Two of them are based on the perception of the standard 4-bar test pattern, of which the *MTDP* is definitely the most promising. It is an evolution of the MRTD concept which takes into account the sampling effects of the imager. The *double slit* method and the *TOD* techniques have more recently been developed. TOD uses triangles as test patterns. TOD is a forced choice technique where the observer responses can be verified, thus obtaining less subjective results. The MRID is still in its infancy. These techniques have benefits which should further be investigated. All listed figures of merit probably will remain in use for further evaluation, which is strongly recommended.

The two objective assessment techniques that are summarised in Table 5.4 both have attractive features. These and similar techniques are still under development. They are listed here in order to document corresponding TG12 activities which respond to the continued interest of the IR community to have fast and reliable assessment techniques without human observer.

Technique	Advantages	Disadvantages
LSF + Noise	extracted from resolution and noise measurements	eye-brain model required; must be calibrated with subjective measurement
Matched filter	suitable for all types of imagers and test patterns	eye-brain model required; must be calibrated with subjective measurement

Table 5.4: ‘Objective’ assessment techniques

This page has been deliberately left blank

Page intentionnellement blanche

Chapter 6

Conclusions and Recommendations

The infrared community has entered an era where staring imagers are becoming the norm and not the exception. Staring array sensors are quickly making their way into target acquisition and surveillance/reconnaissance applications. The large detector characteristics and improved optical quality of these systems make for undersampled image transfer with high sensitivity. The classical MTF and MRT resolution and visual performance parameters, respectively, do not exist for undersampled imagers. In addition, the higher sensitivity of these systems requires that new noise measures be implemented.

TG12 collectively and TG12 member countries have developed and investigated a number of measures and measurement techniques to characterize advanced thermal imagers. These measures and techniques allow assessment of basic, system-relevant sensor parameters, such as spatial resolution and noise, as well as overall sensor performance.

Numerous measures and techniques are available to characterise spatial information transfer and noise in advanced thermal imagers. Also, various figures of merit and measurement techniques are developed to assess the overall device performance. Some of the new figures of merit, such as MTDP, are evolutions of the classical MRTD figure of merit. Other techniques for overall performance assessment use triangles and double-slits as test patterns. These techniques were developed to reduce possible measurement inaccuracies introduced by the subjective nature of assessment techniques which use standard 4-bar test patterns. They have benefits which should further be investigated.

Techniques to assess overall device performance without human observers respond to the continued interest of the IR community to have fast and reliable assessment techniques. Such techniques are still under development.

It is recommended that those STANAGs which address performance assessment of thermal imagers be reviewed. This covers Part III Section 7 of STANAG 4161 on the OTF of thermal imaging systems as well as STANAGs 4347, 4349 and 4350 which are based on MRTD. It is also recommended to standardise definitions and measurement techniques for assessing the noise performance of advanced imagers.

Short term candidates might be the MTDP approach or the NVTherm coupled to DMRT approach. It is the opinion of some TG12 members that an all-objective measurement of resolution and sensitivity and that these measurements be combined to replace the overall visual performance encompassed by MRT. MRT is meaningless in an undersampled imager. In the longer term the forced choice TOD method might be a candidate, which implies however a drastic reconfiguration of the targets and procedures used. Also the double slit method, after careful validation with field experiments, looks promising by its simplicity and ease of modelling.

Summary of Recommendations:

1. Review and update STANAGs 4347, 4349, and 4350 for use with well-sampled imaging systems. There have been numerous improvements in MRT modeling, measurements, and range performance over the past 10 years.
2. Establish a board of experts and an AGGRESSIVE program for developing/evaluating techniques for modeling, measurements, and range performance predictions of undersampled imagers with the goal of drafting STANAG(s) for imager performance. Realize that this is a significant effort that requires nations to participate in laboratory evaluations of techniques, so nations must be willing to

invest time and effort in a development/evaluation program. It should not be the part-time goal of a Technical Group.

3. Note that for some immediate future, there will be mis-applications of the current STANAG methods to undersampled imagers. Staring and scanning infrared sensors are unfairly compared using the current STANAG methods. It is recommended that the MTDP method or the NVTherm/DMRT (dynamic MRTD) method be used until further evaluation can be performed.
4. It is also recommended to standardise definitions and measurement techniques for assessing resolution and sensitivity of advanced imagers.
5. The development of "objective" techniques to assess overall device performance without human observer respond to the continued interest of the IR community and should further be encouraged.

ACKNOWLEDGEMENTS

The work presented and reviewed in this report represents a significant effort made by TG12 and its predecessor group RSG16 of AC/243. The present report is based on a paper that was originally drafted by RSG16. This early work was thoroughly reviewed and updated by TG12. New developments achieved during the last years in TG12 member laboratories were included in order to present the state-of-the-art in the experimental assessment of advanced imagers. We would like to thank all those colleagues who contributed to this document.

REFERENCES

[1] Driggers, R., Wittenstein, W., Willams, D., Bijl, P. and Lopez J.M., "TG12 Report on Modelling of Undersampled Infrared Imaging Systems," to be published as NATO document

[2] STANAG 4161 On the Optical Transfer Function of Imaging Systems, parts I – III, (1979).

[3] STANAG 4161, Part III Section 7 Mechanically Scanned Thermal Imaging Systems, (1981).

[4] see, for instance, Lloyd, J.M., "Thermal Imaging Systems," New York and London, (1975).

[5] Wittenstein W. and Gal, R., "TRM3 progress report," *Proc. SPIE* 4130, (2000).

[6] Vollmerhausen, R., and Driggers, R.G "NVTherm: next generation night vision model;2 Proc. IRIS Passive Sensors, 1, (1999).

[7] Wittenstein, W., "Measurement of the prefilter MTF of undersampled Systems and system characterization". FfO Report 1994/78, 1994

[8] Lettington, A. H. and Hong, Q. H., "A discrete modulation Transfer Function for Focal Plane Arrays". *Infrared Physics*, 34 (1), (1993).

[9] Primot, J., Girard, M. and Chambon. M., "Modulation transfer function assessment for sampled imaging systems: a generalization on the line spread Function". *J. Modern Optics*, 41(7), (1994).

[10] Landeau, St., "Characterization of thermal staring imager with multi-element fractal test targets," *Proc. SPIE* 3377, (1998)

[11] Wittenstein, W., "Performance prediction and experimental assessment of advanced thermal imagers," *Proc. SPIE* 2269, (1994)

[12] de Jong, A.N., Winkel H. and Ghauharali, R.I., "IR sensor performance testing with a double-slit method," *Proc. SPIE* 4372 (2001).

[13] D'Agostino, J.A. and Webb, C.M., "Three-dimensional analysis framework and measurement methodology for imaging system noise," *Proc. SPIE* 1488 (1991).

[14] Scott L. and D'Agostino, J.A., "Application of 3-D noise to MRTD prediction," *Proc. IRIS Passive Sensors Symposium* (1992)

[15] Wittenstein, W. and Fick, W., "Assessment and Measurement of Fixed Pattern Noise in IR Imaging Systems," FfO Note 1991/35, (1991)

[16] Schulz, M. and Caldwell, L., "Nonuniformity correction and correctability of infrared focal plane arrays," *Infrared Phys. Technol.* 36, (1995)

[17] López-Alonso, J.M and Alda, J. "Automatic Classification of Noise for Infrared Images into Processes by means of the Principal Component Analysis," *Proc. SPIE* 4719, (2002) to be published

[18] Mooney, J.M., "Effect of spatial noise on the minimum resolvable temperature of a staring sensor," *Appl. Opt*. 30, (1991)

[19] Wittenstein W., "Summary Record of the 27th meeting of AC/243(Panel IV)RSG16," (1996)

[20] Corluka, "Correctability analysis of infrared focal plane array," DRA document EL/ER1/TR95/83.02.01/108/1.0 (1996)

[21] Lopez Alonso, J.M., Alda, J., "Bad pixel characterisation by means of the principal components analysis," submitted to *Optical Engineering* (2002)

[22] Schulz, M., "*Analysis of Nonuniformity-Corrected IR-Image Data Set*," RSG16 document E/G/34 (1977)

[23] Gross, W., Hierl, Th. and Schulz, M., "Correctability and long term stability of infrared focal plane arrays," *Opt. Eng.*, 38(5), (1999).

[24] STANAG 4349 "On Measurement of the Minimum Resolvable Temperature Difference (MRTD) of Thermal Cameras"

[25] Vollmerhausen, R., Driggers, R. Webb, C.and Edwards, T., "Staring imager minimum resolvable temperature (MRT) measurements beyond the sensor half sample rate," *Opt. Eng.*, 37(6), (1998).

[26] Webb, C., "Dynamic minimum resolvable temperature difference for staring focal plane arrays," *IRIS Passive Sensors Conference*, Johns-Hopkins, March, 1993.

[27] Webb, C. and Halford, C. "Dynamic minimum resolvable temperature difference for staring array imagers," *Opt. Eng.*, 38(5), (1999).

[28] Wittenstein,W. "Minimum temperature difference perceived – a new approach to assess undersampled thermal imagers," *Opt. Eng., 38(5)*, (1999).

[29] Bijl, P.and Valeton, J.M., "TOD, the alternative to MRTD and MRC," *Opt. Eng.* 37(7), (1998).

[30] Bijl, P.and Valeton, J.M., "TOD test method for characterizing electro-optical system performance," *Proc. SPIE* 4372, (2001)

[31] Lange, D.J. de, Valeton, J.M. & Bijl, P. "Automatic characterization of electro-optical sensors with image-processing, using the Triangle Orientation Discrimination (TOD) method," *Proc. SPIE* 4030, (2000).

[32] Hogervorst, M.A. (2001). "Capturing the sampling effects: a TOD sensor performance model," *Proc. SPIE* 4372 (2001)

[33] de Jong, A.N., Roos M.J.J., Kemp R.A.W., "Description of the LION Tester," TNO report FEL-01-A011; January 2001

[34] Bendall, I. and Alonso Lopez, J.M., "Automated objective minimum resolvable temperature difference," *Proc. SPIE* 4030, (2000)

This page has been deliberately left blank

Page intentionnellement blanche

Annex

NATO AC323 (SET/TG12)

ON THE CHARACTERIZATION AND
OPTIMIZATION OF ADVANCED THERMAL IMAGERS

LIST OF MEMBERS

CHAIRMAN

Wittenstein, Wolfgang
FGAN-Forschungsinstitut für Optronik und Mustererkennung (FGAN-FOM)
Gutleuthausstr. 1
D-76275 Ettlingen
Germany
Tel.: +49 7243 992 139
Fax: +49 7243 992 299
E-mail: witte@fom.fgan.de

DENMARK

Nielsen, Niels
Danish Defence Research Establishment (DDRE)
Ryvangs Alle 1
P.O. Box 2715
DK-2100 Copenhagen Ø
Tel.: +45 3 915 1742
Fax: +45 3 929 1533
E-mail: ncn@ddre.dk

Caspersen, Mogens
Danish Defence Research Establishment (DDRE)
Ryvangs Alle 1
P.O. Box 2715
DK-2100 Copenhagen Ø
Tel.: +45 3915 1740
Fax: +45 3929 1533
E-mail: mc@ddre.dk

FRANCE

Blanc-Talon, Jacques, Dr.
DGA/DCE/CTA/DT/GIP
16 bis Ave. Prieur de la Cote d'or
F-94114 Arcueil
Frankreich
Tel.: +33 1 4231 9280
Fax: +33 1 4231 9964
E-mail: blanc@etca.fr

Caniou, Joseph
DGA/DCE/CELAR/GEOS
P.O. 7
35998 Rennes Armees
Tel.: +33 2 9942 9164
Fax: +33 2 9942 9092
E-mail: caniou@celar.fr

Landeau, Stephane, Mr. *
DGA/DSA/SPART/ST/TEC/OP
10, Place George Clemenceau
BP 19
F-92211 Saint Cloud CEDEX
Tel.: +33 1 4771 4257
Fax: +33 1 4771 4370
E-mail: lau@cms.etca.fr

GERMANY

Ischen, Hartmut
FGAN-Forschungsinstitut für Optronik und Mustererkennung (FGAN-FOM)
Gutleuthausstr. 1
D-76275 Ettlingen
Tel.: +49 7243 992 125
Fax: +49 7243 992 299
E-mail: ischen@fom.fgan.de

Schuberth, Wolfgang
FGAN-Forschungsinstitut für Optronik und Mustererkennung (FGAN-FOM)
Gutleuthausstr. 1
D-76275 Ettlingen
Tel.: +49 7243 992 325
Fax: +49 7243 992 299
E-mail: schuberth@fom.fgan.de

ITALY

Licciardello, Giuseppe *
Ministero Difesa
Direzione Generale A.T.
2° Reparto - 6^ Div.
Via Marsala, 104
I-00100 Roma
Tel.: +39 06 4735 5576
Fax: +39 06 484 651

Cini, Andrea, Cdr
Mariteleradar
Viale Italia, 72
I-57100 Livorno
Tel.: +39 0586 238 355
Fax: +39 0586 238 205
E-mail: cinia@marina.difesa.it

NETHERLANDS

de Jong, Arie
TNO - FEL
P.O. Box 96 864
NL-2509 JG The Hague
Tel.: +31 70 374 0456
Fax: +31 70 328 0654
E-mail: dejong@fel.tno.nl

Bijl, Piet, Dr.
TNO-HF
P.O. Box 23
NL - 3769 ZG Soesterberg
Tel.: +31 346 356 277
Fax: +31 346 353 977
E-mail: bijl@tm.tno.nl

SPAIN

Lopez Alonso, Josè Manuel
DGAM/CIDA (MOD)
Arturo Soria, 289
E-28033 Madrid
Tel.: +34 91 302 0640 ext. 1943
Fax: +34 91 766 1648
E-mail:
josema.lopez@homologa.cida.es

USA

Director
US Army Night Vision and Electronic Sensors
Directorate
AMSEL-RD-NV-MSD (Attn: Dr. Ron Driggers)
10221 Burbeck Road, Suite 430
Fort Belvoir, VA 22060-5806

Tel.: +1 703 704 3219
Fax: +1 703 704 1753
E-mail: rdrigger@nvl.army.mil

Williams, Don N.
Commanding Officer
SPAWAR SYSTEMS CENTER
Attn: Code 7405, Don Williams
53560 Hull Street
San Diego, CA 92152-5001

Tel.: +1 619 553 2468
Fax: +1 619 553 6180
E-mail: dnwill@spawar.navy.mil

Bendall, Ike
Commanding Officer
SPAWAR SYSTEMS CENTER
Attn: Code D 754, Bendall
53560 Hull Street
San Diego, CA 92152-5001

Tel.: +1 619 553 2633
Fax: +1 619 553 6842
E-mail: bendall@spawar.navy.mil

This page has been deliberately left blank

Page intentionnellement blanche

REPORT DOCUMENTATION PAGE

1. Recipient's Reference	2. Originator's References	3. Further Reference	4. Security Classification of Document
	RTO-TR-075(II) AC/323(SET-015)TP/21	ISBN 92-837-1095-9	UNCLASSIFIED/ UNLIMITED

5. Originator

Research and Technology Organisation
North Atlantic Treaty Organisation
BP 25, F-92201 Neuilly-sur-Seine Cedex, France

6. Title

Experimental Assessment Parameters and Procedures for Characterisation of Advanced Thermal Imagers

7. Presented at/sponsored by

Task Group SET-015/RTG of the Sensors and Electronics Technology Panel.

8. Author(s)/Editor(s)	9. Date
Multiple	February 2003
10. Author's/Editor's Address	**11. Pages**
Multiple	60

12. Distribution Statement

There are no restrictions on the distribution of this document. Information about the availability of this and other RTO unclassified publications is given on the back cover.

13. Keywords/Descriptors

Bad pixel
Experimental data
Micro-scanned thermal images
Models
MRTD (Minimum Resolvable Temperature Difference)
MTF (Modulation Transfer Function)
Noise characteristics
Procedures
Sampling
Sensitivity
Sensor performance
Spatial resolution
Thermal imagers
Thermal imaging
TOD (Triangle Orientation Discrimination)

14. Abstract

The objective of this study was the development and investigation of experimental assessment parameters and measurement techniques required for characterising advanced staring of micro-scanned thermal imagers. The task group member nations developed and investigated a number of measures and measurement techniques to characterize advanced thermal imagers. They are presented in this report. These measures and techniques allow assessment of basic, system-relevant sensor parameters, such as spatial resolution and noise, as well as overall sensor performance.

This page has been deliberately left blank

Page intentionnellement blanche

NORTH ATLANTIC TREATY ORGANISATION

RESEARCH AND TECHNOLOGY ORGANISATION
BP 25 • 7 RUE ANCELLE
F-92201 NEUILLY-SUR-SEINE CEDEX • FRANCE
Télécopie 0(1)55.61.22.99 • E-mail mailbox@rta.nato.int

DIFFUSION DES PUBLICATIONS
RTO NON CLASSIFIEES

L'Organisation pour la recherche et la technologie de l'OTAN (RTO), détient un stock limité de certaines de ses publications récentes, ainsi que de celles de l'ancien AGARD (Groupe consultatif pour la recherche et les réalisations aérospatiales de l'OTAN). Celles-ci pourront éventuellement être obtenues sous forme de copie papier. Pour de plus amples renseignements concernant l'achat de ces ouvrages, adressez-vous par lettre ou par télécopie à l'adresse indiquée ci-dessus. Veuillez ne pas téléphoner.

Des exemplaires supplémentaires peuvent parfois être obtenus auprès des centres nationaux de distribution indiqués ci-dessous. Si vous souhaitez recevoir toutes les publications de la RTO, ou simplement celles qui concernent certains Panels, vous pouvez demander d'être inclus sur la liste d'envoi de l'un de ces centres.

Les publications de la RTO et de l'AGARD sont en vente auprès des agences de vente indiquées ci-dessous, sous forme de photocopie ou de microfiche. Certains originaux peuvent également être obtenus auprès de CASI.

CENTRES DE DIFFUSION NATIONAUX

ALLEMAGNE
Streitkräfteamt / Abteilung III
Fachinformationszentrum der Bundeswehr, (FIZBw)
Friedrich-Ebert-Allee 34
D-53113 Bonn

BELGIQUE
Etat-Major de la Défense
Département d'Etat-Major Stratégie
ACOS-STRAT-STE – Coord. RTO
Quartier Reine Elisabeth
Rue d'Evère, B-1140 Bruxelles

CANADA
DSIGRD2
Bibliothécaire des ressources du savoir
R et D pour la défense Canada
Ministère de la Défense nationale
305, rue Rideau, 9e étage
Ottawa, Ontario K1A 0K2

DANEMARK
Danish Defence Research Establishment
Ryvangs Allé 1, P.O. Box 2715
DK-2100 Copenhagen Ø

ESPAGNE
INTA (RTO/AGARD Publications)
Carretera de Torrejón a Ajalvir, Pk.4
28850 Torrejón de Ardoz - Madrid

ETATS-UNIS
NASA Center for AeroSpace Information (CASI)
Parkway Center
7121 Standard Drive
Hanover, MD 21076-1320

FRANCE
O.N.E.R.A. (ISP)
29, Avenue de la Division Leclerc
BP 72, 92322 Châtillon Cedex

GRECE (Correspondant)
Defence Industry & Research General Directorate
Research Directorate
Fakinos Base Camp
S.T.G. 1020
Holargos, Athens

HONGRIE
Department for Scientific Analysis
Institute of Military Technology
Ministry of Defence
H-1525 Budapest P O Box 26

ISLANDE
Director of Aviation
c/o Flugrad
Reykjavik

ITALIE
Centro di Documentazione Tecnico-Scientifica della Difesa
Via XX Settembre 123a
00187 Roma

LUXEMBOURG
Voir Belgique

NORVEGE
Norwegian Defence Research Establishment
Attn: Biblioteket
P.O. Box 25, NO-2007 Kjeller

PAYS-BAS
Royal Netherlands Military Academy Library
P.O. Box 90.002
4800 PA Breda

POLOGNE
Armament Policy Department
218 Niepodleglosci Av.
00-911 Warsaw

PORTUGAL
Estado Maior da Força Aérea
SDFA - Centro de Documentação
Alfragide
P-2720 Amadora

REPUBLIQUE TCHEQUE
DIC Czech Republic-NATO RTO
VTÚL a PVO Praha
Mladoboleslavská ul.
Praha 9, 197 06, Česká republika

ROYAUME-UNI
Dstl Knowledge Services
Kentigern House, Room 2246
65 Brown Street
Glasgow G2 8EX

TURQUIE
Millî Savunma Başkanliği (MSB)
ARGE Dairesi Başkanliği (MSB)
06650 Bakanliklar - Ankara

AGENCES DE VENTE

NASA Center for AeroSpace Information (CASI)
Parkway Center
7121 Standard Drive
Hanover, MD 21076-1320
Etats-Unis

The British Library Document Supply Centre
Boston Spa, Wetherby
West Yorkshire LS23 7BQ
Royaume-Uni

Canada Institute for Scientific and Technical Information (CISTI)
National Research Council
Acquisitions
Montreal Road, Building M-55
Ottawa K1A 0S2, Canada

Les demandes de documents RTO ou AGARD doivent comporter la dénomination "RTO" ou "AGARD" selon le cas, suivie du numéro de série (par exemple AGARD-AG-315). Des informations analogues, telles que le titre et la date de publication sont souhaitables. Des références bibliographiques complètes ainsi que des résumés des publications RTO et AGARD figurent dans les journaux suivants:

Scientific and Technical Aerospace Reports (STAR)
STAR peut être consulté en ligne au localisateur de ressources uniformes (URL) suivant:
http://www.sti.nasa.gov/Pubs/star/Star.html
STAR est édité par CASI dans le cadre du programme NASA d'information scientifique et technique (STI)
STI Program Office, MS 157A
NASA Langley Research Center
Hampton, Virginia 23681-0001
Etats-Unis

Government Reports Announcements & Index (GRA&I)
publié par le National Technical Information Service
Springfield
Virginia 2216
Etats-Unis
(accessible également en mode interactif dans la base de données bibliographiques en ligne du NTIS, et sur CD-ROM)

Imprimé par Groupe d'imprimerie St-Joseph inc.
(Membre de la Corporation St-Joseph)
1165, rue Kenaston, Ottawa (Ontario), Canada K1G 6S1

NORTH ATLANTIC TREATY ORGANISATION

RESEARCH AND TECHNOLOGY ORGANISATION
BP 25 • 7 RUE ANCELLE
F-92201 NEUILLY-SUR-SEINE CEDEX • FRANCE
Telefax 0(1)55.61.22.99 • E-mail mailbox@rta.nato.int

DISTRIBUTION OF UNCLASSIFIED RTO PUBLICATIONS

NATO's Research and Technology Organisation (RTO) holds limited quantities of some of its recent publications and those of the former AGARD (Advisory Group for Aerospace Research & Development of NATO), and these may be available for purchase in hard copy form. For more information, write or send a telefax to the address given above. **Please do not telephone**.

Further copies are sometimes available from the National Distribution Centres listed below. If you wish to receive all RTO publications, or just those relating to one or more specific RTO Panels, they may be willing to include you (or your organisation) in their distribution.

RTO and AGARD publications may be purchased from the Sales Agencies listed below, in photocopy or microfiche form. Original copies of some publications may be available from CASI.

NATIONAL DISTRIBUTION CENTRES

BELGIUM
Etat-Major de la Défense
Département d'Etat-Major Stratégie
ACOS-STRAT-STE – Coord. RTO
Quartier Reine Elisabeth
Rue d'Evère, B-1140 Bruxelles

CANADA
DRDKIM2
Knowledge Resources Librarian
Defence R&D Canada
Department of National Defence
305 Rideau Street, 9th Floor
Ottawa, Ontario K1A 0K2

CZECH REPUBLIC
DIC Czech Republic-NATO RTO
VTÚL a PVO Praha
Mladoboleslavská ul.
Praha 9, 197 06, Česká republika

DENMARK
Danish Defence Research Establishment
Ryvangs Allé 1, P.O. Box 2715
DK-2100 Copenhagen Ø

FRANCE
O.N.E.R.A. (ISP)
29 Avenue de la Division Leclerc
BP 72, 92322 Châtillon Cedex

GERMANY
Streitkräfteamt / Abteilung III
Fachinformationszentrum der Bundeswehr, (FIZBw)
Friedrich-Ebert-Allee 34
D-53113 Bonn

GREECE (Point of Contact)
Defence Industry & Research General Directorate
Research Directorate
Fakinos Base Camp
S.T.G. 1020
Holargos, Athens

HUNGARY
Department for Scientific Analysis
Institute of Military Technology
Ministry of Defence
H-1525 Budapest P O Box 26

ICELAND
Director of Aviation
c/o Flugrad
Reykjavik

ITALY
Centro di Documentazione Tecnico-Scientifica della Difesa
Via XX Settembre 123a
00187 Roma

LUXEMBOURG
See Belgium

NETHERLANDS
Royal Netherlands Military Academy Library
P.O. Box 90.002
4800 PA Breda

NORWAY
Norwegian Defence Research Establishment
Attn: Biblioteket
P.O. Box 25, NO-2007 Kjeller

POLAND
Armament Policy Department
218 Niepodleglosci Av.
00-911 Warsaw

PORTUGAL
Estado Maior da Força Aérea
SDFA - Centro de Documentação
Alfragide
P-2720 Amadora

SPAIN
INTA (RTO/AGARD Publications)
Carretera de Torrejón a Ajalvir, Pk.4
28850 Torrejón de Ardoz - Madrid

TURKEY
Millî Savunma Başkanliği (MSB)
ARGE Dairesi Başkanliği (MSB)
06650 Bakanliklar - Ankara

UNITED KINGDOM
Dstl Knowledge Services
Kentigern House, Room 2246
65 Brown Street
Glasgow G2 8EX

UNITED STATES
NASA Center for AeroSpace Information (CASI)
Parkway Center
7121 Standard Drive
Hanover, MD 21076-1320

SALES AGENCIES

NASA Center for AeroSpace Information (CASI)
Parkway Center
7121 Standard Drive
Hanover, MD 21076-1320
United States

The British Library Document Supply Centre
Boston Spa, Wetherby
West Yorkshire LS23 7BQ
United Kingdom

Canada Institute for Scientific and Technical Information (CISTI)
National Research Council
Acquisitions
Montreal Road, Building M-55
Ottawa K1A 0S2, Canada

Requests for RTO or AGARD documents should include the word 'RTO' or 'AGARD', as appropriate, followed by the serial number (for example AGARD-AG-315). Collateral information such as title and publication date is desirable. Full bibliographical references and abstracts of RTO and AGARD publications are given in the following journals:

Scientific and Technical Aerospace Reports (STAR)
STAR is available on-line at the following uniform resource locator:
http://www.sti.nasa.gov/Pubs/star/Star.html
STAR is published by CASI for the NASA Scientific and Technical Information (STI) Program
STI Program Office, MS 157A
NASA Langley Research Center
Hampton, Virginia 23681-0001
United States

Government Reports Announcements & Index (GRA&I)
published by the National Technical Information Service
Springfield
Virginia 22161
United States
(also available online in the NTIS Bibliographic Database or on CD-ROM)

Printed by St. Joseph Print Group Inc.
(A St. Joseph Corporation Company)
1165 Kenaston Street, Ottawa, Ontario, Canada K1G 6S1

ISBN 92-837-1095-9